Physics of high-intensity high-energy Particle Beam Propagation in open Air and outer-space Plasmas

Andre Gsponer

Independent Scientific Research Institute Box 30, CH-1211 Geneva-12, Switzerland e-mail: isri@vtx.ch

ISRI-82-04.22 January 3, 2019

Abstract

This report is a self-contained and comprehensive review of the physics of propagating pulses of high-intensity high-energy particle beams in pre-existing or self-generated plasmas. The first part is a systematic overview of the theory pertaining to propagation, plasma self-generation, energy/current-losses, and stability of such pulses. The second part reviews the major full-scale propagation experiments which have been carried out, in atmospheric and outer-space plasmas, to assess the validity of theoretical models. It is found that the data available on these experiments demonstrate that range and stability are in agreement with theory. In particular, stable self-pinched propagation of high-current beams in the atmosphere is possible over distances on the order of several Nordsieck lengths.

Contents

1	Introduction		5	
2	Some preliminary definitions			
3	Part	ticle beam propagation in a vacuum or a tenuous plasma	9	
	3.1	Neutral beam in a vacuum	9	
	3.2	Charged beam in a vacuum	10	
4	Particle beam propagation in a dense gas or plasma			
	4.1	Charged beam in a plasma: the Bennett pinch	12	
	4.2	Effect of magnetic fields: neutral plasma beams	18	
	4.3	Charged beam in a dense gas or plasma: Nordsieck equation	19	
5	Inje	ction of a high-power beam into the atmosphere	26	
	5.1	Plasma generation by a particle beam	26	
	5.2	Conductivity generation and critical beam current	30	
	5.3	Beam head erosion and ohmic losses	34	
6	Stability of propagating high-power beams			
	6.1	General considerations on beam stability	37	
	6.2	Microinstabilities	42	
		6.2.1 Two-stream instability	42	

		6.2.2	Weibel (or micro-filamentation) instability	44
		6.2.3	Discussion of microinstabilities	46
	6.3	Macroi	nstabilities	47
		6.3.1	Electrostatic kink instability	48
		6.3.2	Electromagnetic kink (or "resistive hose") instability	50
		6.3.3	Macrostability of a beam penetrating a neutral gas	52
		6.3.4	Macrostability of beams with rounded radial profiles	54
		6.3.5	Discussion of macroinstabilities	57
7	Disc	ussion o	of theoretical prospect	58
8	Disc	ussion o	f beam propagation experiments	61
9	Neut	ral par	ticle beam propagation experiments	63
	9.1	Neutra	particle beam technology development	63
		9.1.1	The ion source	64
		9.1.2	The injector	64
		9.1.3	The accelerator	65
		9.1.4	The beam focusing and steering optics	66
		9.1.5	The neutralizing cell	66
		9.1.6	Summary	67
	9.2	BEAR	and GTA at Los Alamos National Laboratory	67
	9.3	Emergi	ng neutral beam technologies	69
10	Chai	rged pai	rticle beam propagation experiments	73
	10.1	ATA at	Lawrence Livermore National Laboratory	73
	10.2	RADL	AC at Sandia National Laboratory	77
	10.3	LIA-10	and LIA-30 at Arzamas-16	80
	10 4	PHERM	MEX at Los Alamos National Laboratory	81

	10.5 Proton and muon beams	82
11	Conclusion	84
	Bibliography	84

List of Figures

4.1	The pinch effect	16
4.2	Beam expansion for various particles	21
4.3	Effective beam range versus momentum for various particles	22
5 1	Propagation of a pinched beam	27
3.1	riopagation of a pinched beam	21
5.2	Coordinate system used in describing the propagating beam	28
5 3	Beam neck profile	24

Chapter 1

Introduction

This report deals in a comprehensive manner with theoretical and experimental plasma-physics and accelerator-physics research which have been actively followed or done by the author over the past twenty-five years, that is starting from approximately the time of the beginning of the construction of the "Advanced Test Accelerator" (ATA) at the Lawrence Livermore National Laboratory, and of the creation of the "Accelerator Technology" (AT) division at the Los Alamos National Laboratory.

In order to understand the relevance of the key experiments, which started to give significant data in the mid-1980s, it is important to understand the theory underlying the numerous plasma-physics effects at work when a high-intensity beam-pulse of particles propagates in a background gas or through the atmosphere. Since there is no published text book or monograph covering this subject in a systematic manner, Chapters 2 to 7 attempt to make a synthesis of numerous published articles and many informal reports which deal with one or another aspect of this theory. As shown by the bibliography, this meant studying many papers published over the past fifty years, often dealing only indirectly with the subject, in order to extract the pertinent information necessary to make a consistent theoretical model.

In the second part of the report, Chapters 8 to 10, the focus is on the accelerator facilities and the beam propagation experiments which are significant for the purpose of establishing the feasibility of generating suitable high-intensity high-energy particle beams, and of propagating them in outer-space plasmas or through the atmosphere. The difficulty, here, is that the openly available data is more of a qualitative than quantitative nature, which is precisely why a thorough understanding of the plasma-physics pertinent to these experiments is so important. In

these chapters, which deal with technologies at the frontier of the state-of-the-art, an effort is made to refer to the implications of the most advanced theoretical ideas and technologies, in order to show how much the possible future engineering-development of high-power particle beam generation/propagation technology still depends on ongoing research.

While we said that there appears to be no published text book or monograph covering the subject of this report in a systematic manner, there is a growing number of excellent books available on the physics of charged particle beams and their applications. The books by J.D. Lawson [1], R.B. Miller [2], S. Humphries Jr. [3, 4], and M. Reiser [5], are possibly the most useful in the context of the present report.

As the information and research summarized in this report extend over so many years, there are many people to thank for their direct and indirect contributions to it. While I cannot mention all of them, I wish in particular to thank my former colleagues at CERN (where this work started): Claude Bovey, Steve Geer, Peter Jenni, Pierre Lefèvre, Claude Metzger, Dieter Moehl, Emilio Picasso, Monique et Raymond Séné, Peter Sonderegger, Charling Tao, Daniel Treille, and Horst Wachsmuth; as well as Frank Barnaby and Bhupendra Jasani at SIPRI (where the first part of this report was written); and last but not least, Jean-Pierre Hurni at ISRI.

¹One exception appears to be the lecture notes prepared by Prof. K.E. Woehler, Department of Physics, Naval Postgraduate School, Monterey, CA, for his course PH 4959 — Physics of directed energy weapons: Part I, Particle beam weapons (March 1981) 120 pp; Part II, Particle accelerators (March 1981) 60 pp. However, the level and scope of these lectures are more elementary and less comprehensive than those of the present report.

Chapter 2

Some preliminary definitions

A particle beam pulse may be thought of as an ensemble of moving particles whose trajectories constitute a "bundle." The diameter of this bundle is small compared with its length, and the trajectories generally make a small angle with the "axis." The complete description of the evolution of such a system of interacting particles, especially if they propagate through a gas or plasma, is in general very complicated. However, in many cases, the beam pulse can be characterized statistically by the RMS (i.e., "root mean squared") values of its radius, length, angular spread, energy spread, etc. A good description is then provided by the so-called *envelope equations* giving the RMS radius (or length) of the pulse as a function of time or propagation distance.

A most important concept specifically related to particle beams is that of *emittance*, which can be considered as a measure of the disorder in the motion of the particles relative to the average motion of the beam [6].¹ In the general case it is necessary to distinguish between the transverse and longitudinal emittances, i.e., ϵ_{\perp} and ϵ_{\parallel} , which will be defined in the first section of the next chapter. Since an emittance is basically the product of the extent of a spatial distribution along a given direction by an angular spread, i.e., a length times an angle, it is generally measured in units of "meter-radian."

A concept that is related to beam emittance is that of beam *brightness*, i.e., current divided by angular beam spread, which means that low-emittance implies high-brightness, and vice versa. Both concepts are often used interchangeably to qualify a high-power directed beam, but we will use only the concept of emittance

¹There are several, essentially equivalent, definitions of emittance. In this report we use the so-called "RMS emittance" which is both the most convenient and the most frequently used in our context.

in the theoretical sections of this report.

In order to simplify the calculations, the usual treatment generally assumes that \tilde{v}_{\perp} and \tilde{v}_{\parallel} , the RMS values of the random components of the transverse (or perpendicular) and longitudinal (or parallel) velocities, are small compared with the mean longitudinal drift velocity $v = \beta c$:

$$\tilde{v}_{\perp}^2 \ll \beta^2 c^2 \ , \ \tilde{v}_{\parallel}^2 \ll \beta^2 c^2 \ .$$
 (2.1)

This is the *paraxial approximation* in which the particle's trajectories deviate only slightly from parallel straight lines. In such a model, the beam particle momentum p, total energy W, and kinetic energy K, are slowly changing parameters with the longitudinal distance. With $\gamma = 1/\sqrt{1-\beta^2}$ the Lorentz factor,

$$p = \gamma \beta mc$$
 , $W = \gamma mc^2$, $K = (\gamma - 1)mc^2$. (2.2)

In the case of charged particle beams, we will see that the paraxial approximation is equivalent to the statement that the *effective beam current* I_E generating the electromagnetic self-fields is small compared with the *Alfvén current* I_A , a characteristic current defined as [7, 8]:

$$I_A = 4\pi\epsilon_0 c^2 \frac{p}{q} \approx 17000 \frac{\beta \gamma}{Z} \text{ [Ampere]} \approx \frac{pc}{30Z} \frac{\text{[e-Volt]}}{\text{[e-Ohm]}}$$
 (2.3)

where q = Z|e| is the electric charge of the beam particles.

In the discussion of problems like beam-plasma interaction and stability, the most convenient radial scale is not the RMS radius $\tilde{a} = \sqrt{\langle r^2 \rangle}$, but the scale radius a defined such that

$$J_B(0) = \frac{I_B}{\pi a^2} {2.4}$$

where $J_B(r)$ is the areal current density and I_B the total beam current.

We will use a cylindrical coordinate system with radial distance $r=\sqrt{x^2+y^2}$, azimuthal angle θ , and longitudinal distance z. In the beam frame, we will replace the longitudinal variable z by a time coordinate τ which is zero at the beam head and equal to $\Delta \tau$, the pulse duration, at the tail-end.

In the following two chapters we will review the envelope equations for neutral and charged particle beams. We will assume homogeneous and constant background conditions, and neglect transient effects and instabilities. Then, in Chapter 5, we will examine the transient effects at the head of a charged beam when it is fired into a initially neutral gas such as the atmosphere which is turned into a plasma by the beam. Finally, in Chapter 6, before concluding the theoretical part of this report, we will examine the main possible instabilities affecting the propagation of such a beam.

Chapter 3

Particle beam propagation in a vacuum or a tenuous plasma

3.1 Neutral beam in a vacuum

In the absence of collisions between the particles, the individual trajectories of neutral particles propagating in a vacuum are all straight lines. The envelope equations can then directly be derived from kinematics [9]. For a beam pulse with axial symmetry, the RMS radius \tilde{a} , and the RMS half-length $\tilde{\ell}$, are given of by:

$$\tilde{a}'' = \frac{\epsilon_{\perp}^2}{\tilde{a}^3} \ , \ \tilde{\ell}'' = \frac{\epsilon_{\parallel}^2}{\tilde{\ell}^3} \ . \tag{3.1}$$

In these envelope equations, the primes denote derivation with respect to the longitudinal coordinate z. The constant ϵ_{\perp} and ϵ_{\parallel} are the RMS transverse and longitudinal emittances which characterize the random distribution of the particles in the beam. Specifically

$$\epsilon_{\perp}^2 = \tilde{a}^2 \frac{(\tilde{v}_{\perp})^2 - v^2(\tilde{a}')^2}{v^2} , \quad \epsilon_{\parallel}^2 = \tilde{\ell}^2 \frac{(\tilde{v}_{\parallel})^2 - v^2(\tilde{\ell}')^2}{v^2} .$$
 (3.2)

As ϵ_{\perp} and ϵ_{\parallel} are constants of motion, they can be measured most conveniently at the point where the beam envelope forms a waist. At such a point $\tilde{a}'=0$ or $\tilde{\ell}'=0$, and

$$\epsilon_{\perp} = \tilde{a}\tilde{\alpha} \ , \ \epsilon_{\parallel} = \frac{\tilde{\ell}}{\gamma^2} \frac{\Delta W}{W} \ .$$
 (3.3)

¹For an alternate derivation of this equation, which applies to any beam without collisions in the absence of external forces, see [1, p.187].

where, in the paraxial limit, $\tilde{\alpha}$ is the RMS angular spread and $\Delta W/W$ the RMS energy spread of the beam. The emittances ϵ_{\perp} and ϵ_{\parallel} are thus characteristic of the beam quality: a small transverse emittance corresponds to a well collimated small angular divergence beam, and a small longitudinal emittance to a short pulse with a small energy spread.

For possible applications for space-based beam weapon systems, the general solution of (3.1) has one essential feature: for a given emittance, and at a fixed distance z from the accelerator generating the beam, the minimum beam spot size is inversely proportional to its initial radius \tilde{a}_0 , i.e.,

$$\tilde{a}_{min} = z \frac{\epsilon_{\perp}}{\tilde{a}_0} \ . \tag{3.4}$$

This minimum is achieved for $\tilde{a}'_0 = \tilde{a}_0/z$ and shows that the critical parameter in focusing the beam is its emittance and not just its angular spread or radius. Similarly, the longitudinal emittance determines the minimum duration of beam pulses, and is thus an essential parameter for compressing the beam into short pulses at the target. According to (3.4), in order to focus a neutral beam into a 1 m radius at 1000 km, one would, for example, need a beam with an initial radius of 20 cm and an emittance of 2×10^{-7} m·rad. An accelerator with such an emittance, and a focusing system for such a beam, have been developed at the Los Alamos National Laboratory in the USA [10].

3.2 Charged beam in a vacuum

When a charged particle beam is launched into a vacuum, the beam will tend to spread apart because of its emittance and the effect of the Coulomb repulsion between like charges, which is particularly strong if the beam energy is low. However, for relativistic beams, this is not the main problem with propagation in a complete vacuum: when an unneutralized beam leaves the accelerator, the accelerator becomes charged with the opposite sign, pulling the beam particles back and causing them to decelerate. Let us examine the importance of these effects.

In the paraxial limit the radial electrostatic force on a particle within a beam at a distance r from the axis is

$$F_e = 2\frac{W}{r} \frac{I_B(r)}{I_A} \tag{3.5}$$

²These remarkable simple results are obtained by finding the general solution $\tilde{a}(z)$ of (3.1), and minimizing it with respect to $\tilde{a}'(0)$, the focusing angle of the beam.

where $I_B(r)$ is the total current flowing within the radius r. This outward-directed force is partially compensated for by the inward-directed pinch force due to the azimuthal magnetic field generated by the beam current within this radius:

$$F_m = -2\beta^2 \frac{W}{r} \frac{I_B(r)}{I_A} \ . \tag{3.6}$$

As $\beta^2 < 1$, the net force $F_e + F_m$ is outward-directed, and causes the beam to spread apart. By equating this force to the transverse acceleration force $m\gamma\ddot{r} = m\gamma\beta^2c^2r''$, we get the radial equation [11], [1, p.134]

$$r'' = \frac{2}{\beta^2 \gamma^2} \frac{I_B}{I_A} \frac{1}{r} = \frac{\kappa}{r} , \qquad (3.7)$$

where κ is called the *perveance*, i.e., a measure of the extent to which a beam is influenced by its space charge. The distance over which a beam has to propagate in order for it radius to double is then approximately given by [11], [1, p.136]:

$$z_2 \approx a_0 \beta \gamma \sqrt{I_A/I_B} . {3.8}$$

With an initial radius of $a_0 = 20$ cm, a kinetic energy of 500 MeV, and a current of 100 mA, this distance would be about 2600 km for electrons, but only 100 m for a proton beam with the same characteristics. But this is estimated from radial beam divergence alone. In fact, as there is no return current the particle will also be slowed down under the action of the longitudinal restoring force due to charging up of the spacecraft launching the beam. This effect puts a limit to the range of charged particles in a vacuum. In first approximation [12]

$$z_{max} \approx a_0 \frac{(\gamma^{2/3} - 1)^{3/4}}{\gamma^{1/2}} \sqrt{\frac{I_A}{2I_B}} ,$$
 (3.9)

so that the ranges of the above beams would be less than about 1800 km for electrons, and 100 m for protons. This calculation alone would tend to rule out the use of charged particle streams as possible beam weapons in a vacuum. However, as will be examined now, if such beams were injected into outer space, which is in fact a dilute plasma and not a vacuum, the situation can be very different.

While equation (3.7) corresponds to the motion of an electron at the edge of a beam (r = a), the radial envelope equation combining the effects of the emittance as defined in [9], and those of the electro-magnetic self-fields, is [13]:

$$\tilde{a}'' = \frac{\epsilon_{\perp}^2}{\tilde{a}^3} + \frac{1}{\beta^2 \gamma^2} \frac{I_B}{I_A} \frac{1}{\tilde{a}} . \tag{3.10}$$

Compared to (3.7), we see that there is no factor "2" in the perveance term because the radial variable is the RMS radius \tilde{a} rather then r. This is typical of the many essentially equivalent beam envelope equations which can be written down, and which differ by numerical factors on the order of 2.

Chapter 4

Particle beam propagation in a dense gas or plasma

4.1 Charged beam in a plasma: the Bennett pinch

Charged particle beams for use as directed energy weapons are in general injected either into the atmosphere for ground- and aircraft-based systems, or into a plasma for space-based systems. In the case of atmospheric systems, the beam will enter an initially neutral atmosphere and, by ionizing the air, turn it into a plasma along the beam path. In the case of outer-space systems, the plasma will be the ionosphere for near earth orbiting systems, or the interstellar environment. In all cases, the transient phenomena occurring at the head of a beam pulse are complicated. We will thus concentrate first on infinitely long beams in the paraxial approximation. Similarly, we will assume that the plasma can be sufficiently well described for our purpose by a scalar electric conductivity σ given by

$$\sigma = \frac{e^2}{\nu} \frac{n_e}{m_e} \tag{4.1}$$

where ν is the collision frequency, m_e the electron rest mass, and n_e the number density of the conductivity electrons.

In order to appreciate the relative importance of the plasma background for beam propagation, it is sufficient to compare the plasma density n_e to the beam particle density n_b . On the beam axis, according to (2.4),

$$n_b(0) = \frac{1}{e\beta c} \frac{I_B}{\pi a^2} \ . \tag{4.2}$$

For example, in the case of a relativistic beam with $I_B=100$ mA and a=20 cm, $n_b=1.6\times 10^4$ cm⁻³. In comparison, in the ionosphere between an altitude of 100 to 2000 km, the electron number density n_e is on the same order or larger. Therefore, plasma effects cannot be ignored.

The first effect of a plasma background is that, because of quasi-neutrality, the excess charge locally introduced by the passage of the beam will tend to be neutralized on a time scale τ_e set by the plasma conductivity, i.e., by definition, the *electric diffusion time* of the plasma:

$$\tau_e = \frac{\epsilon_0}{\sigma} \ . \tag{4.3}$$

As a result, the space charged force (3.5) will be reduced to a value

$$F_e = 2(1 - f_e) \frac{W}{r} \frac{I_B(r)}{I_A}$$
 (4.4)

where f_e is the charge neutralization fraction.

The actual physical processes involved at the microscopic level are different depending upon the sign of the electric charge of the beam particles. For an electron beam, the electric field will quickly expel the plasma electrons and the neutralization will be provided by the positive ions left within the beam. Assuming the ions not to be able to move significantly during the passage of the beam pulse, the maximum charge neutralization fraction will be $f_e = |n_i/n_b|$ in cases where $n_i < n_b$. In the case of a proton beam, electrons from the plasma surrounding the beam will be attracted into the beam region. The neutralizing fraction can be one even when $n_e < n_b$. The fact that the charge neutralizing particles have very different masses means that the transient phenomena and stability conditions can be different in the two beams. However, in dense plasma, i.e., when $n_e \approx n_i > n_b$, most properties will be similar. In particular, f_e will essentially be one for beam pulses of duration longer than τ_e and radius smaller than c/τ_e .

The second main effect of a plasma background is that a return current can be established. This current is driven by E_z , the longitudinal electric field induced by the beam. From Faraday's law of induction

$$E_z = -\frac{1}{\pi \epsilon_0 c^2} \frac{\partial}{\partial t} (\mathcal{L} I_E) , \qquad (4.5)$$

where I_E is the effective current driving the electromagnetic self-fields, and \mathcal{L} a dimensionless inductance. For axially symmetric beams

$$\mathcal{L} \approx \frac{1}{4}\ln(1 + \frac{b^2}{a^2})\tag{4.6}$$

where b is the maximum radius out to which the plasma background is significantly affected by the beam. For instance, in beam-generated plasmas, b is normally determined by the extent of induced breakdown around the beam head. Typically, $b/a \approx 10$, i.e., $\mathcal{L} \approx 1$. At the boundary of this region the conductivity becomes too small to ensure quasineutrality. The charge imbalance from the beam is conducted to this surface, which is thus the path along which the beam current not neutralized by the plasma current is returned to the accelerator. From Ohm's law, $J = \sigma E$, the longitudinal component of the plasma current is then

$$I_P = \pi a^2 \sigma E_z = -\tau_m \frac{\partial}{\partial t} (\mathcal{L} I_E)$$
(4.7)

where

$$\tau_m := \frac{\sigma}{\epsilon_0} \frac{a^2}{c^2} \tag{4.8}$$

is by definition the *magnetic diffusion time* of the plasma. From (4.5) it turns out that the plasma current will in effect decrease the beam current and thus reduce the magnetic pinch force. This is usually written as

$$F_m = -2(1 - f_m)\beta^2 \frac{W}{r} \frac{I_B(r)}{I_A}$$
(4.9)

where $f_m := |I_P/I_B|$ is the magnetic neutralization fraction. Because E_z is a function of the beam current and shape variations, the plasma current, and thus f_m , will be largest at the beam head. Within the pulse, f_m will decrease to zero on a time scale set by the magnetic diffusion time.¹

Assuming f_e and f_m to be independent of r, the envelope equation including the plasma effects is then [13]

$$\tilde{a}'' + \frac{I_E}{I_A} \frac{1}{\tilde{a}} = \frac{\epsilon_\perp^2}{\tilde{a}^3} \tag{4.10}$$

where I_E is the effective current associated with the net electromagnetic force on the beam:

$$I_E = I_B \left((1 - f_m) - \frac{1}{\beta^2} (1 - f_e) \right) .$$
 (4.11)

When $f_e = f_m = 0$, i.e., in a vacuum where $I_E = -I_B \beta^{-2} \gamma^{-2}$, equation (4.11) is obviously equivalent to (3.10).

The effective current I_E contains charge imbalance as well as true beam and plasma currents. It can have both signs, and the forces can either tend to separate

¹This will be discussed in more details in Chapter 5.

or, on the contrary, to pinch the beam. When I_E is positive, a stationary solution with $\tilde{a}'' = \tilde{a}' = 0$ is possible. This is the *Bennett pinch* solution, and in that case (4.10) gives [11, 14]:

$$\tilde{a} = \epsilon_{\perp} \sqrt{\frac{I_A}{I_E}} = a_B \quad . \tag{4.12}$$

From (4.11) we see that a_B , the *Bennett pinch radius* defined by (4.12), is minimum for $f_e = 1$ and $f_m = 0$. In that case $I_E = I_B$, the pinch force is maximum, and the beam is fully pinched. The Bennett pinch solution exists, however, only in the paraxial limit. This can be seen from (4.12) and (3.2) which imply

$$\frac{I_E}{I_A} < \frac{\tilde{v}_\perp^2}{v^2} \ll 1$$
 (4.13)

In a Bennett pinch, the beam particles perform harmonic motion around the beam axis. The angular frequency of the rotation is a function of r and is called the betatron frequency $\omega_{\beta}(r)$. By equating the net force $F_e + F_m$ to the centrifugal force $\gamma m \omega_{\beta}^2 r$, and by averaging over the beam current density, one finds from (4.4) and (4.9) that the mean azimuthal velocity is given by

$$\tilde{v}_{\theta}^2 = \overline{\omega_{\beta}^2 r^2} = \beta^2 c^2 \frac{I_E}{I_A} \tag{4.14}$$

which is independent of the beam profile. In the general case, the betatron frequency ω_{β}^2 is distributed between zero and a maximum

$$\omega_{\beta m}^2 = \omega_{\beta}^2(0) = 2\beta^2 \frac{c^2}{a^2} \frac{I_E}{I_A} , \qquad (4.15)$$

which is also independent of the beam profile. In the special case of a beam with a constant current density out to a radius a, the betatron frequency is constant and equal to the maximum given by (4.15).

For propagating self-pinched beams, the most natural equilibrium density profiles are those corresponding to a Maxwellian (i.e., Gaussian) transverse energy distribution [15].

Possible equilibria include filamentary current flows along the axis, but the simplest realistic example is the so-called *Bennett distribution* [14]

$$J_B(r) = \frac{I_B}{\pi a^2} \left(1 + \frac{r^2}{a^2} \right)^{-2} . \tag{4.16}$$

The RMS radius of this distribution diverges logarithmically. However, both theory and experiment [16, 17] that indicate a Bennett profile are not valid for

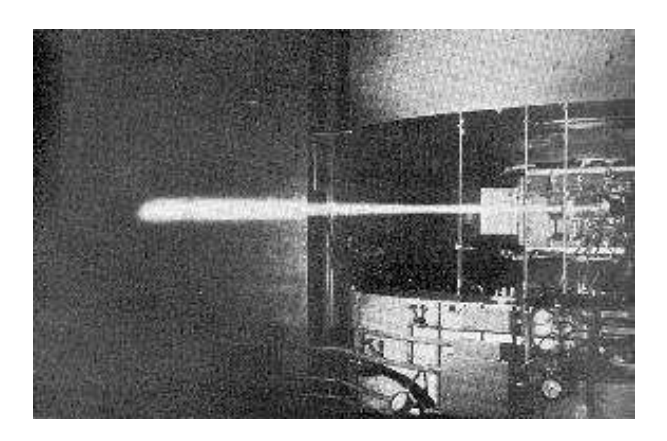


Figure 4.1: The pinch effect. The photograph, taken in the early 1950s at the Argonne cyclotron (near Chicago), shows the glow produced when sending the full deuteron beam into the atmosphere. Because of ionization the air near the beam is turned into a plasma which keeps the beam from expanding radially under the effect of Coulomb repulsion between like-charged particles: This is the "Bennett pinch effect," first described by Willard H. Bennet in 1934 to explain focusing effects and breakdown in the residual gas of high-voltage electronic tubes, and later applied to the propagation of interstellar and interplanetary selffocussed beams of particles, such as proton streams traveling from the sun towards the earth. As the beam loses energy and intensity because of interactions with atmospheric nitrogen and oxygen nuclei, plasma generation becomes less efficient and the beam progressively expands: This is the "Nordsieck effect," after the name of Arnold Nordsieck who is generally credited for having first explained this expansion. Ultimately, when the plasma effects become to weak to pinch the beam, it breaks-up. This happens at a propagation distance on the order of the so-called "Nordsieck length."

 $r\gg a$. In practice, the current profile is often considered to be truncated at r=2a. This yields $\tilde{a}=1.006~a$.

In a beam with the Bennett profile (4.16), the betatron frequency ω_{β}^2 is is uniformly distributed between zero and the maximum given by (4.15).

The significance of the Bennett pinch is that when a beam is injected in a gas or plasma sufficiently dense to suppress the effect of the space charge repulsion, the beam may pinch down to a minimum constant radius and propagate over large distances. In particular, because the plasma background provides a means for carrying the return current, the range is no more strictly limited as it was in the case of charged beams in vacuum. The limit to the propagation distance will now be set by scattering, energy loss, instabilities, etc., as will be seen in Section 4.3.

The fact that the net charge transported by a beam pulse traveling through a plasma is equal to the charge of the beam itself, even when the beam is launched from a ground plane, is not an obvious result. It is, however, correct, even when the plasma is generated within the pulse by beam-gas interactions [18].

The Bennett pinch is important in many areas of science and technology. In particular, it is important for understanding interplanetary particle streams [7, 14] and studying the ionosphere with beams launched from rockets [19] or the space shuttle [20]. It has many applications in thermonuclear fusion research and has been envisaged as a means for accumulating high energy electrons in large rings in outer space. Such rings could be used to store energy and subsequently generate synchrotron radiation or free-electron laser optical beams [21]. Finally, for endo-atmospheric beam weapons, the pinch effect provides the means for radially confining charged particle beams.

The Bennett pinch condition $I_E>0$ requires $f_e>1/\gamma^2$ when $f_m=0$. For high energy beams, i.e., $\gamma=10$ to 10^4 , this condition is easily satisfied, even in very low density plasmas. This allows the transport of beams with current densities higher than the plasma density by a factor γ^2 .

The practicality of this method for stable propagation of beams over large distances in a low pressure atmosphere was demonstrated for electrons in 1972 [22]. For beams such as those considered at the end of the previous paragraph, the pinch effect would provide an ultimate theoretical range of many thousands of kilometers. However, the practical use of such beams in outer space will, in fact, be limited by the effect on them of Earth's magnetic field. On the other hand, in a full density atmosphere, the possibility of experimentally demonstrating the feasibility of using the pinch effect to propagate a charged-particle beam had to wait for the construction of large scale facilities at several laboratories [23, 24].

4.2 Effect of magnetic fields: neutral plasma beams

The region above the atmosphere in which an orbiting charged particle beam weapon might be deployed contains plasma and magnetic fields of both solar and terrestrial origin. The plasma may enable electron or proton beams to pinch and propagate over large distances, but the magnetic fields would strongly affect the beam trajectory in most cases.

In a homogeneous magnetic field B the radius of curvature of a particle of charge q is

 $R = \frac{p}{qB} . {(4.17)}$

Hence, for an electron or proton with momentum $p=1~{\rm GeV/c}$ and in a field of 0.3 Gauss typical of Earth's geomagnetic field, R would be $\approx 110~{\rm km}$. In the absence of any other effect, such a deflection would be a small correction for an endo-atmospheric system with a range of a few kilometers. However, for an outer-space system with a required range of several thousands of kilometers, the beam would spiral much as it did in low-energy beam experiments performed on the space shuttle [20].

For beams without current neutralization (i.e., $f_m=0$), the effect of an external magnetic field is essentially the same as that on the beam particles taken individually. In that case, (4.17) applies directly to the beam as a whole, which has been verified experimentally [25]. On the other hand, if $f_m \neq 0$, the overall effect of an external magnetic field on a beam would be smaller, and would vanish in the extreme case of a fully current-neutralized beam.

This phenomenon is most easily understood in the ideal case of a *neutral* plasma beam consisting of co-moving electrons and ions. Since electrons and ions are deflected in opposite directions they create a polarization electric field. This field exactly cancels the force of the external magnetic field and the beam continues undeflected, loosing, however, particles from the polarization layers [26]. This effect has been investigated experimentally for a charge-neutral beam consisting of electrons and protons [27]. For such a beam, the effective current (4.11) is evidently zero. The envelope equation (4.10) reduces then to that of neutral beam and, in the absence of the pinch effect, the neutral plasma beam would expand through the effect of its emittance [28].

A neutral plasma beam, also called *plasmoïd beam*, would thus be an alternative to a neutral particle beam for outer space systems. The main problem is to generate such a plasmoïd beam with a sufficiently small emittance for the range to be useful, and to overcome the problem of the beam losses at the boundary layers.

In an atmosphere with a pressure of about 1 Torr, stable propagation conditions with $f_e = f_m = 1$ were discovered in early electron beam experiments, first in the United States [29, 30], and later in the Soviet Union [12]. In these experiments, the current neutralization was provided by slowly counterstreaming plasma electrons. The fact that such a configuration is stable and unaffected by an external magnetic field would make it attractive, in principle, for propagating a beam in a reduced density channel. However, the beam is not pinched, and would thus quickly spread apart because of collisions with the gas molecules.

4.3 Charged beam in a dense gas or plasma: Nord-sieck equation

When a beam propagates in a dense gas or plasma, the collisions with the electrons and nuclei result in a loss of energy by the beam particles, and eventually a loss in beam current when particles can effectively be removed from the beam by interactions with nuclei. Furthermore, by increasing the angular and energy spread of the beam, the collisions lead to a continuous increase in both transverse and longitudinal emittance. In the paraxial approximation the full radial envelope equation taking energy loss and scattering into account is as follows [13, 16]:²

$$\tilde{a}'' + \frac{I_E}{I_A} \frac{1}{\tilde{a}} + \frac{\tilde{a}'W'}{\beta^2 W} = \frac{1}{\tilde{a}^3 p^2} \left(p_0^2 \epsilon_{\perp 0}^2 + \int_0^z \tilde{a}^2 p^2 \, d\psi^2 \right) . \tag{4.18}$$

This result is obtained from kinetic theory which shows [16] that a self-pinched beam subject to gas scattering evolves to a state in which its current density takes the form of the Bennett distribution (4.16), which is a similarity solution of the Fokker-Planck equation with $\tilde{a} \approx a$ for $r \leq \mathcal{O}(a)$.

In (4.18) all parameters are, in general, a function of the propagation distance z. The third term on the left hand side, for instance, is the contribution to radial expansion coming from the decrease of the beam's particle energy W(z). The right hand side corresponds to the increase in transverse emittance because of Coulomb multiple scattering in the background gas. In agreement with Liouville's theorem [1], the emittance enters this formula through the product $p\epsilon$ which is the relativistic invariant, conserved emittance for a beam of varying energy. In first approximation, the multiple scattering angle is given by Rossi's formula [31,

²The theories developed in these two papers differ by some non-essential factors of "2." What matters is that they are used consistently when compared to experimental data.

p.67]³
$$d\psi^{2} = \left(\frac{E_{s}}{\beta cp}\right)^{2} \frac{dz}{X_{0}}$$
 (4.19)

where $E_s = \sqrt{4\pi/\alpha}\,m_ec^2 \approx 21.2$ MeV and $X_0 = 4\pi r_e^2 \rho N_A/A$ is the radiation length of the medium, i.e., $X_0 \approx 300.5$ m for air at standard temperature and pressure (STP).⁴

The total energy of the beam particles as a function of z is given by the equation

$$W' := \frac{dW}{dz} = -S(\beta) - \frac{W}{X_0} + qE_z . {(4.20)}$$

The first term is the Bethe's stopping power and corresponds to energy losses by ionization and excitation of the gas molecules [31]. This loss is a slowly varying function of energy and S equal 2 to 3 keV/cm in air at STP for 1 GeV single-charged particles. The second term is present only for electron beams and corresponds to bremsstrahlung radiation losses [31]. (Bremsstrahlung emission is negligible for particles of mass heavier than electrons). The third term corresponds to the ohmic losses in the induced longitudinal electric field. These losses which are associated with the charge and current neutralization process are concentrated in the head of the beam where they contribute to heating the plasma electrons.

The beam current decreases because of collisions with nuclei. In the case of proton beams, both inelastic and elastic nuclear collisions will effectively remove particles from the beam. Therefore, in that case, the effective beam current (4.11) will vary with z as

$$I_E(z) = I_E(0) \exp(-z/X_n)$$
 (4.21)

where X_n is the nuclear collision length, about 500 m in air at STP for high energy proton beams. In the case of electron beams, the pronounced statistical character of bremsstrahlung radiation losses will result in a wide energy spread for propagations over distances of the order of one radiation length. The implication of such a large increase in longitudinal emittance is that particles with energies less than half the mean beam energy will in fact "evaporate" from the beam, thus leaving behind a reduced current beam [33]. A calculation based on Bethe and Heitler's theory of straggling in bremsstrahlung emission [31] indicates that this effect would account for a 30% loss in beam current for a high energy electron beam propagating over one radiation length.

³Rossi's formula provides a convenient first approximation for analytical calculations of the kind done in this section. For more precise calculations, especially for beams of relatively low-momentum particles, it is better to use Molière's theory as formulated by Bethe [32].

 $^{^4\}alpha=1/137$ is the fine-structure constant, and $r_e=e^2/m_ec^2$ the classical electron radius.

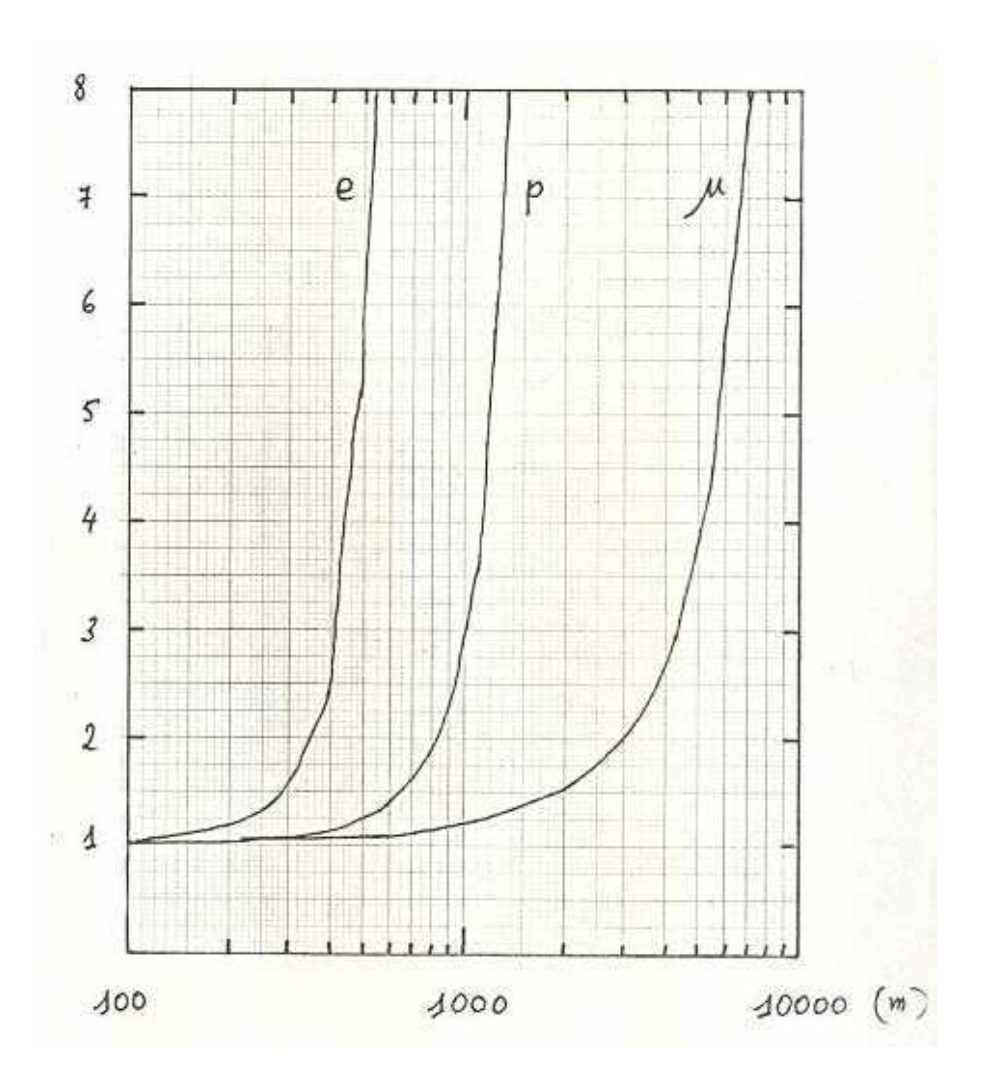


Figure 4.2: Beam expansion for various particles. The radial expansion of a beam of intensity $I_B=10~\rm kA$ and momentum $P_B=10~\rm GeV/c$, calculated by integrating numerically the full radial envelope equation taking all energy losses and scattering effects into account, is plotted as a function of propagation distance in air at STP. The e-folding range, also called the Nordsieck length, defined as the distance at which the beam radius has expanded by a factor of $e\approx 2.718$, is of about about 400, 1000, or 4000 meter for an electron, proton, or muon beam, respectively.

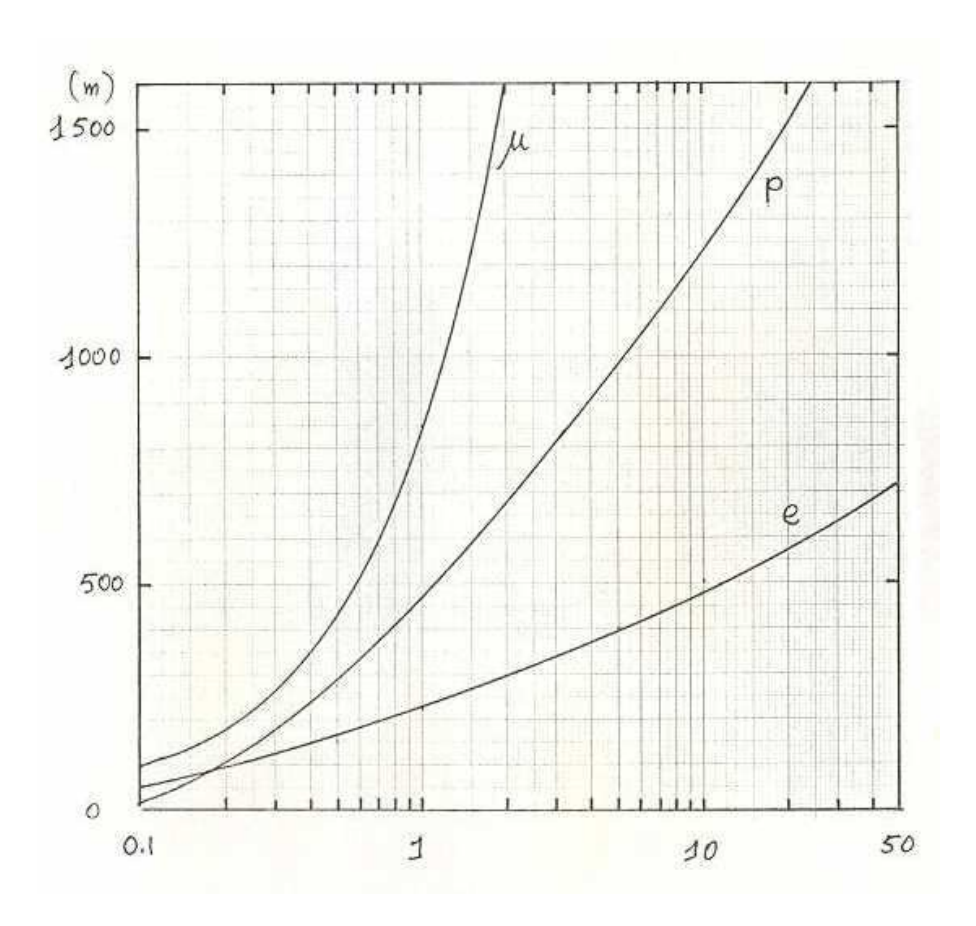


Figure 4.3: Effective beam range versus momentum for various particles. The effective range, defined as the distance at which the beam radius has expanded by a factor of $2e\approx 5$, is plotted as a function a beam momentum in GeV/c. For a beam intensity $I_B=10~\rm kA$ the range in air at STP of a single 1 GeV/c electron, proton, or muon beam pulse is of about 200, 500, or 800 m, respectively. For a 10 GeV/c pulse the effective range increases to about 500 or 1200 m for an electron or proton beam, and about 6000 m for a muon beam (see Figure 4.2).

The solution of (4.18) has generally to be found numerically. However, considerable insight can be gained in the quasistatic limit $\tilde{a}'' = \tilde{a}' \approx 0$, where (4.18) becomes

$$\tilde{a}^2 p^2 \frac{I_E}{I_A} = \int_0^z \tilde{a}^2 p^2 \, d\psi^2 \ , \tag{4.22}$$

which can trivially be rewritten as

$$\frac{d}{dz}\ln\left(\tilde{a}^2p^2\frac{I_E}{I_A}\right) = \tilde{a}^2p^2\frac{I_A}{I_E}\frac{d\psi^2}{dz} \ . \tag{4.23}$$

If one takes Rossi's multiple scattering formula (4.19), and uses the definition of the Alfvén current, this equation becomes the so-called *Nordsieck equation* [13, 16]:

$$\frac{d}{dz}\ln(P_E\tilde{a}^2) = \frac{P_N}{P_E}\frac{1}{\beta^2 X_0} , \qquad (4.24)$$

where $P_E = I_E(z)p(z)c/e$ is the effective beam power, and $P_N = cE_s^2/e^2 = (c/r_e)(4\pi/\alpha)m_ec^2 \approx 15\times 10^{12}~{\rm W} = 15~{\rm TW}$ is a physical constant: the *Nordsieck power*. The remarkable property of this approximate envelope equation is that the radial expansion of a relativistic beam in a gas is a function of only two variables: the radiation length X_0 which characterizes the medium, and the effective power P_E which characterizes the beam.

The Nordsieck equation can be solved explicitly for several cases of interest. For instance, for high-energy *proton beams*, the dominant beam power loss comes from the decrease in beam current due to nuclear interactions: $P_E(z) \approx P_0 \exp(-z/X_n)$. Then, for relativistic proton beams such that $\beta \approx 1$,

$$a = a_0 \exp \frac{1}{2} \left(\frac{z}{X_n} + \frac{P_N X_n}{P_0 X_0} \left(\exp(z/X_n) - 1 \right) \right) . \tag{4.25}$$

On the other hand, for high-energy *electron beams*, the dominant effect is energy loss by bremsstrahlungs: $P_E(z) \approx P_0 \exp(-z/X_0)$. Thus, as $\beta \approx 1$,

$$a = a_0 \exp \frac{1}{2} \left(\frac{z}{X_0} + \frac{P_N}{P_0} \left(\exp(z/X_0) - 1 \right) \right) . \tag{4.26}$$

In both cases, the Nordsieck power P_N plays an important role. For $P_0 < P_N$, the radial expansion is very fast and the beam cannot propagate over sizable distances.

For $P_0 > P_N$, however, the e-folding range, also called the *Nordsieck length*, defined as the distance over which the beam radius expands by a factor of $e \approx 2.718$, becomes independent of initial beam power. It is about $z_N \approx 2X_n \approx 1000$ m for protons and $z_N \approx 2X_0 \approx 600$ m for electrons in air at STP. The implication is that for a beam to propagate, its total effective power has to be on

the order of $P_N=15$ TW, but any further increase in beam power would not substantially increase its range.

In the low-energy limit, i.e., $P_0 < P_N$, the beam will propagate less than one radiation or nuclear interaction length. One can therefore assume that $z \ll X_0$ for electrons, and $z \ll X_n$ for protons, to find that in first approximation the Nordsieck length for both an electron or a proton beam is then given by

$$z_N \approx 2 \frac{P_0}{P_N + P_0} X_0 . {(4.27)}$$

For example, the maximum power of the 10 kA, 50 MeV, ATA beam is $P_0 = 0.5$ TW. Since the Nordsieck power is $P_N = 15$ TW, and the radiation length $X_0 \approx 300$ m in air at STP, the typical propagation length of a single ATA beam pulse should be on the order of $z_N \approx 20$ m.

In order to check the validity of these conclusions we have written a computer program to solve (4.18) in the general case, modeling all physical effects such as multiple scattering, energy losses, etc., as precisely as possible.

First, we have solved (4.18) for 10 GeV/c momentum, 10 kA beams of electrons, protons and muons in air at STP. This corresponds to an initial beam power $P_0 = 6.6 P_N$, and the results are shown in Figure 4.2. Second, we have calculated the effective range, defined as the distance at which the beam radius has expanded by a factor of $2e \approx 5$, as a function of momentum for 10 kA beams of these particles, see Figure 4.3.

The *e*-folding range of the *proton beam* is about 1 km, as expected. But it is only 400 m for the *electron beam*. (See Figure 4.2.) This discrepancy is the result of the approximation made in deriving the Nordsieck equation (4.24) and of neglecting straggling.

The *muon beam*, which would be much more difficult to produce in practice than an electron or proton beam, is included for comparison. As bremsstrahlungs and nuclear interactions are negligible for these particles, the muon beam range is of course much larger. (See Figures 4.2 and 4.3.)

The range of proton beams in air is thus strictly limited by the nuclear interaction length, and that of electron beams by the radiation length. However, as these lengths depend directly upon the atmospheric density, the corresponding ranges will increase in proportion to the decrease in atmospheric density.

Finally, in order to compare the beam expansion theory given in this section to the data, and therefore to validate the extrapolations given in Figures 4.2 and 4.3, we have simulated and found good agreement with the beam expansion

measurements given in reference [17]. In these measurements, the ASTRON induction linear accelerator of the Lawrence Livermore National Laboratory was used to propagate a 250 ns, 0.85 kA, 5 MeV electron beam pulse over a distance up to 16 m in reduced density nitrogen. This agreement can be also be used to predict with some confidence the propagation characteristics of the 10 kA, 50 MeV, ATA beam. It is then found that one *e*-folding beam-radius increase corresponds to a propagation distance of about 20 m in sea-level air, in excellent agreement with the analytical estimate given by equation (4.27), and that the beam radius increases to about ten times its initial value after propagating a distance of about 35 m.

Chapter 5

Injection of a high-power beam into the atmosphere

5.1 Plasma generation by a particle beam

In a endo-atmospheric system, except when the beam is launched into the ionosphere or a pre-formed plasma channel, the beam will, in general, be injected into initially un-ionized air. At the very head of a beam pulse, there is thus no background plasma and therefore, both f_e and f_m are zero. The beam head, therefore, expands at a rate governed by the net radial electromagnetic force, emittance and scattering. However, as the beam ionizes the air, a plasma of increasing density builds up and, as plasma currents start flowing, the space charge gets progressively neutralized. When $I_E=0$, that is when $\gamma^2(f_m\beta^2-f_e)=1$ according to (4.11), the net electromagnetic force changes sign, and the beam stops expanding out and starts pinching in.

During the self-pinching of the beam, both the radius a and the effective beam current I_E change rapidly, and this happens while the beam current I_B , which in practice has a finite rise-time, increases. As a result, a strong electric field is induced. This field, given by (4.5), accelerates the plasma electrons, which, as they gain sufficient energy, start ionizing the gas as well. The rate of neutralization of the beam thus increases, until it levels off as the decreasing beam radius approaches an equilibrium radius given by the Bennett pinch relation (4.12) with $f_e \approx 1$. At this point, the induced electric field becomes very small and, the plasma current I_P , after having gone through a maximum, starts decreasing according to (4.7). Finally, for a sufficiently long pulse, after the plasma current has completely decayed, the beam becomes fully pinched.

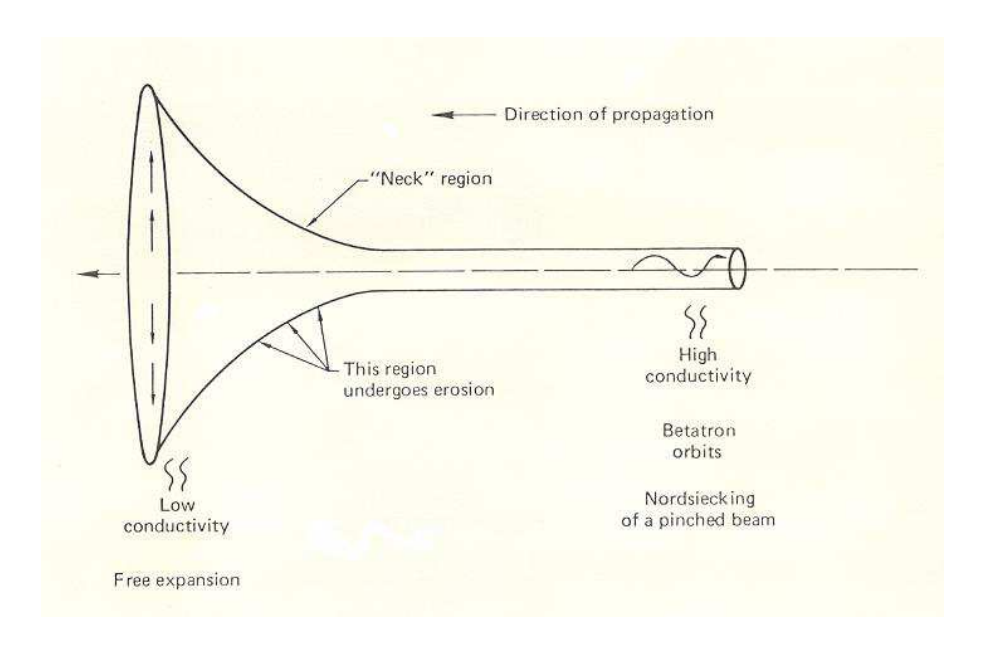


Figure 5.1: *Propagation of a pinched beam.* The diagram shows a propagating beam indicating the pinching, necking, and freely expanding regions. In the high-conductivity pinched (also called "Nordsiecking") region the particles perform betatron orbits with a slowly increasing radius. In the neck region the beam expands and undergoes erosion as particles are lost as a result of weakening pinch forces. Finally, in the low-conductivity free expansion region where the plasma effects are not sufficient to pinch the beam, the particles move away from each other because of Coulomb repulsion.

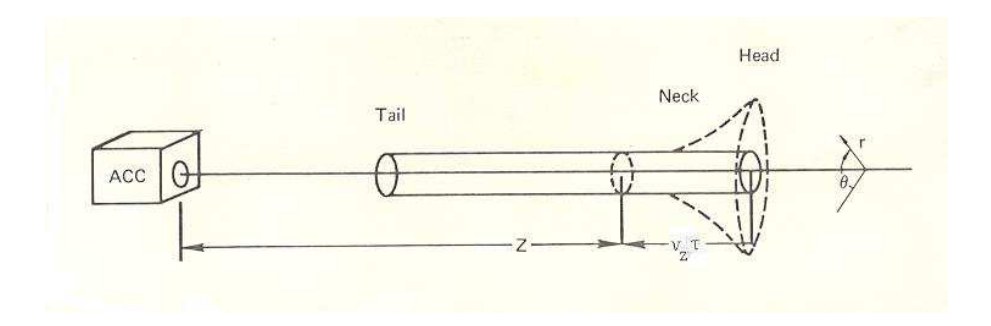


Figure 5.2: Coordinate system used in describing the propagating beam. The variable z is the distance from the accelerator to a point within a beam pulse, while the variable τ is the time such that the distance from this point to the beam head is equal to $v_z\tau$, where v_z is the longitudinal velocity of the beam's particles.

As a result of this process, the beam pulse takes on a characteristic "trumpet" shape, and can be divided into four distinct regions; the expanding beam head, the neck region in which E_z and f_m are maximum, the body in which $f_e \approx 1$ and Nordsieck's equation becomes a good approximation of (4.18), and finally the tail where $f_e = 1$ and $f_m \approx 0$. (See Figure 5.1.)

The description of this process requires an equation for the plasma electron density n_e and temperature T_e so that the conductivity σ , and thus τ_e and τ_m can be calculated. Furthermore, in order that all quantities can be expressed self-consistently, an equation relating the various fields and currents is needed. This last equation is called the *circuit equation*.

These equations, which describe quantities directly related to the penetration distance of the beam into the gas, are best written down as a function of the following variable:

$$\tau = t - z/\beta c \tag{5.1}$$

au has the dimension of the time and is a fixed label for a given particle within the pulse, provided this particle does not move relative to the beam head. For the beam head au=0, and for the tail-end, au is simply the beam pulse duration. (See Figure 5.2.)

The circuit equation has to be derived from the full set of Maxwell's equations. However, provided that a similarity assumption is made on the radial profile of the various charge and current distributions, the circuit equation takes a remarkably simple form. First, it has to be noticed that because the plasma electrons are mostly generated directly by the beam, n_e , and thus σ , will have radial distributions close to that of I_B . Second, as a consequence, the plasma current I_P will also have a

distribution similar to I_B [34] and f_m , just like f_e , will be independent of r. The natural radial distribution function to take (for all quantities) is that of a Bennett profile (4.16), and in that case the circuit equation takes the form [35]:

$$I_E = I_B - \tau_e a^2 \frac{\partial}{\partial \tau} (\frac{I_E}{a^2}) - \tau_m \frac{\partial}{\partial \tau} (\mathcal{L}I_E) - \tau_e \tau_m \frac{\partial^2}{\partial^2 \tau} (\mathcal{L}I_E) . \tag{5.2}$$

The second term on the right is the current associated with the charge neutralization process and is thus important only at the beam head and neck. The third term is the plasma return current I_P . The last term is the displacement current which can be generally neglected, except at the very head of the beam. In this equation, τ_e and τ_m are calculated from the on-axis values of σ .

The exact form of the equation giving the plasma conductivity depends considerably upon the chemical composition and the pressure of the gas. The general form of the plasma electron density equation is as follow [36]:

$$\frac{\partial}{\partial \tau} n_e = \beta c \frac{S}{w} + \nu_i n_e - \nu_a n_e - \alpha_r n_e^2 . \tag{5.3}$$

The first term is the direct beam ionization rate where $S(\beta)$ is the Bethe's stopping power, and w=33.7 eV for air, the energy required to create one electron-ion pair. The second source term corresponds to ionization avalanche in the induced electrical field at the beam head. The third corresponds to conductivity electron loss by attachement to various molecules, and the last one to losses by molecular dissociative recombination. In general, the rates ν_i , ν_a , and the recombination coefficient α_r , depend on the gas pressure, the electric field, and the plasma temperature. Therefore, for a real gas like air, a complete description would require a set of rate equations coupling the various populations of molecular and atomic nitrogen, oxygen, water, etc., in various states of ionization, to the beam source terms. This leads to the development of complicated phenomenological models [37].

In order to calculate the conductivity σ , the collision frequency ν of the conductivity electrons with the plasma is also needed. This is the sum of two terms:

$$\nu = \nu_e(T_e, n_g) + \nu_i(T_e, n_g)$$
 (5.4)

The first term is the electron-neutral momentum transfer collision frequency, and the second one the electron-electron collision frequency [36]. For dilute plasmas, in which n_e is less than a few per cent of the molecular gas density n_g , the second term can generally be neglected.

Finally, a last equation giving the plasma temperature T_e is also required. This is generally done by phenomenologically relating T_e to E_z [37, 38], or by

constructing an equation relating the conductivity σ to Joule heating, thermal cooling by conduction and energy loss as free energy [39].

In conclusion, the plasma chemistry involved in the calculation of the conductivity is generally rather complicated. However, for short pulses in dense gases such as air in the pressure range of 0.1 to 1 atmosphere, a good first approximation is obtained by assuming an average plasma temperature of $T_e \approx 2 \, \text{eV}$ and keeping dissociative recombination with oxygen as the main cause of electron loss. In that case [38]

$$\alpha_r \approx 10^{-8} \text{ cm}^3 \text{s}^{-1}$$
 and $\nu \approx 1.8 \times 10^{-7} n_q \text{ s}^{-1}$, (5.5)

which gives a collision frequency $\nu \approx 4.86 \times 10^{12}~{\rm s}^{-1}$ for air at STP, which corresponds to $n_q \approx 3.4 \times 10^{18}~{\rm cm}^{-3}$.

The four equations (4.18), (4.20), (5.2) and (5.3) constitute a full set of equations providing a complete 1-dimensional description of the propagation of a beam pulse in a gas or plasma. The main assumptions leading to these equations are the paraxial approximation, the description of the plasma by a scalar conductivity, and the similarity of all radial distributions. Whereas these coupled equations cannot be solved in general without a computer, their main features and implications for endo-atmospheric beam weapons can be derived by making some approximations.

5.2 Conductivity generation and critical beam current

When a high-current beam pulse is injected into air at full atmospheric pressure, the avalanche ionization term can be neglected and (5.3) can be solved explicitly to give n_e as a function of τ . With the further approximations (5.5), one can calculate the plasma conductivity σ and thus the magnetic diffusion time τ_m :

$$\tau_m = \tau_M \frac{\exp(2\frac{I_B}{I_G} \frac{\tau}{\tau_M}) - 1}{\exp(2\frac{I_B}{I_G} \frac{\tau}{\tau_M}) + 1}$$

$$(5.6)$$

where

$$\tau_M = 2a\sqrt{\frac{\pi}{\nu}} \frac{r_e}{\alpha_r} \frac{I_B}{I_G} \tag{5.7}$$

and

$$I_G = \frac{1}{4} \frac{e\nu w}{r_e S} \approx 7.2 \text{ kA}$$
 (5.8)

with r_e the classical radius of the electron and e the electron charge. I_G , the conductivity generation current, which controls the rate of conductivity generation, is a critical current independent of pressure, and of beam parameters for $\beta \approx 1$, i.e., relativistic beams for which Bethe's stopping power $S(\beta)$ is nearly constant.

The value of I_G is typically on the order of 10 kA. τ_M , the asymptotic value of τ_m , increases with the beam radius and current, as well as with a reduction in atmospheric pressure. For pulses that are long relative to $\tau_M I_G/I_B$, τ_m will thus approach τ_M , whereas for short pulses, or at the beam head (5.6) reduces to

$$\tau_m(\tau) \approx \frac{I_B}{I_G} \tau$$
 (5.9)

We will now make the drastic approximation that both \tilde{a}' and \tilde{a}'' can be neglected in (4.18). This approximation is only valid in the quasistatic limit leading to Bennett's or Nordsieck's equations. However, this hypothesis corresponds approximately to the situation in which a beam head leaves the exit window of an accelerator to penetrate into the atmosphere. Finally, we will assume a beam current I_B with an infinitely short rise-time. Under these conditions, neglecting the displacement current, the circuit equation (5.2) can be solved. With (5.9), the effective current is then

$$I_E = I_B \left(1 - \frac{1}{\beta^2} \left(1 + \lambda \frac{\tau^2}{\tau_p^2} \right)^{-1/\lambda} \right)$$
 (5.10)

where

$$\lambda = 2\mathcal{L}\frac{I_B}{I_G} \tag{5.11}$$

and

$$\tau_p = \frac{a}{c} \sqrt{2 \frac{I_G}{I_R}} \quad . \tag{5.12}$$

It is now possible to calculate various quantities, and in particular the plasma current I_P which turns out to be maximum at $\tau = \tau_p$. The region where I_P is maximum can be defined as the beam neck. However, as τ_p is calculated for a beam with infinitely short rise-time, it does not give the absolute position of the beam neck. Nevertheless, τ_p can be used to calculate relative quantities, and in particular the neutralization fractions at the point where the beam is pinching. This is because plasma phenomena are dominant in the beam head, and to first approximation independent of rise-time: the conductivity becomes smaller as the rise-time is reduced, but the inductive electric fields becomes greater, thus resulting in the same plasma current when I_B reaches its maximum [40].

For $\tau = \tau_p$, the charge neutralization is

$$f_{ep} = 1 - (1 + \lambda)^{-1 - 1/\lambda}$$
 (5.13)

At the pinch point, f_e is thus equal to $1 - 1/e \approx 0.63$ for $\lambda \ll 1$ and about one for $\lambda \gg 1$. The corresponding result for the current neutralization fraction is

$$f_{mp} = \frac{\lambda}{\beta^2} (1 + \lambda)^{-1 - 1/\lambda} . \tag{5.14}$$

The maximum current neutralization fraction is thus small as long $\lambda \ll 1$, but close to one for $\lambda \gg 1$. Consequently, in order for a beam to be well pinched, which requires $f_m < 1$, one has to have $\lambda < 1$, or, explicitly

$$I_B < \frac{1}{2f}I_G . ag{5.15}$$

As $I_G \approx 10$ kA, this is a rather strong limitation on the beam current. Indeed, for particle beam weapons, current in excess of I_G are required for endo-atmospheric systems, and this creates some problems.

These analytical results are in good agreement with detailed computer calculations which do not assume a constant beam radius [41]. In these calculations the radius of the beam at the neck is well approximated by

$$a_n \approx a_\infty \left(1 + \frac{I_B}{I_C}\right) \tag{5.16}$$

which shows that for $I_B > I_G$, the neck radius is proportional to the beam current.

The pinch condition is not the only one leading towards the requirement of small current neutralization fractions. We will see, for instance, that a beam is also more likely to be unstable when $f_m > 0.5$. Therefore, it turns out that I_G corresponds to a *critical beam current* setting an upper limit to the current of a beam pulse sent into the atmosphere.

It is interesting to notice that the maximum current neutralization fraction calculated with (5.14) is in reasonable agreement with the result of detailed computer calculations [38, 41]. For example, in the case of a 10 kA, 50 MeV beam pulse such as produced by the ATA accelerator at the Lawrence Livermore Laboratory, we find $f_{mp} = 0.50$, whereas the computer calculations [38] predicts $f_{mp} = 0.4$. In that case a = 0.5 cm and $b \approx 10$ cm; therefore $\mathcal{L} = 1.5$ and $\lambda = 4.2$.

The maximum current neutralization fraction (5.14) is independent of pressure. But, as pressure is reduced, the ionization by avalanche can no longer be neglected.

The result (5.14) is then a lower bound to the maximum current neutralization fraction. For example, for the above mentioned ATA accelerator beam injected into air at 0.1 atmospheric pressure, the computer calculations [38] give $f_{mp} = 0.8$.

The maximum value of the longitudinal electric field which appears during the self-pinching of the beam can be calculated from the circuit equation. In first approximation one finds:

$$E_{z,max} = \frac{1}{4\pi\epsilon_0 c^2} 2\frac{c}{a} \sqrt{\mathcal{L}} I_B . \qquad (5.17)$$

In the head region where E_z is maximum, a is of the order of b. Thus:

$$E_{z,max} = 2500 \frac{I_B}{h} \text{ [V/m]} .$$
 (5.18)

For beam currents of 10 to 100 kA and head radii of 3 to 30 cm, we find fields of the order of 10 MV/m. This maximum electric field is quite large and is approximately independent of the beam current. This is because the beam head radius becomes proportional to the beam current when $I_B > I_G$, as it is shown by computer calculations [41].

In the body of a beam pulse long enough for τ_m to reach its asymptotic value (5.7), the circuit equation becomes a linear equation with constant coefficients. It can then be solved easily. In particular, when neglecting τ_e , the plasma current is

$$I_P = -I_B \exp(-\frac{\tau}{\mathcal{L}\tau_m}) f_{mp} . {(5.19)}$$

For the previous examples, the plasma current decay time $\mathcal{L}\tau_m$ would be of 10 ns and 35 ns at the respective pressures of 1 and 0.1 atmosphere. Thus, if f_m is large at the pinch point, the current neutralization fraction will remain almost constant throughout the pulse, provided its length is less than $\mathcal{L}\tau_m$.

A last case of importance is that of a beam pulse injected into a plasma of such a density that its conductivity remains constant. (This is in particular the case when $\nu_e > \nu_m$ in (5.4) so that σ becomes the Spitzer conductivity [42], which implies that the conductivity given by (4.1) should be divided by a factor $\ln \Lambda \approx 10$.) In that situation, because the plasma density is high, plasma currents can start flowing right from the very beginning of the pulse. The current neutralization is therefore almost complete at the beam head, and (5.19) with $f_{mp} = 1$ will give the plasma current throughout the pulse. Because of this large current neutralization, the beam head will not be pinched even though charge neutralization is complete. Therefore, a pulse injected into a plasma or preionized background will also have an expanded head, and beam pinching then occurs as the longitudinal plasma current decays.

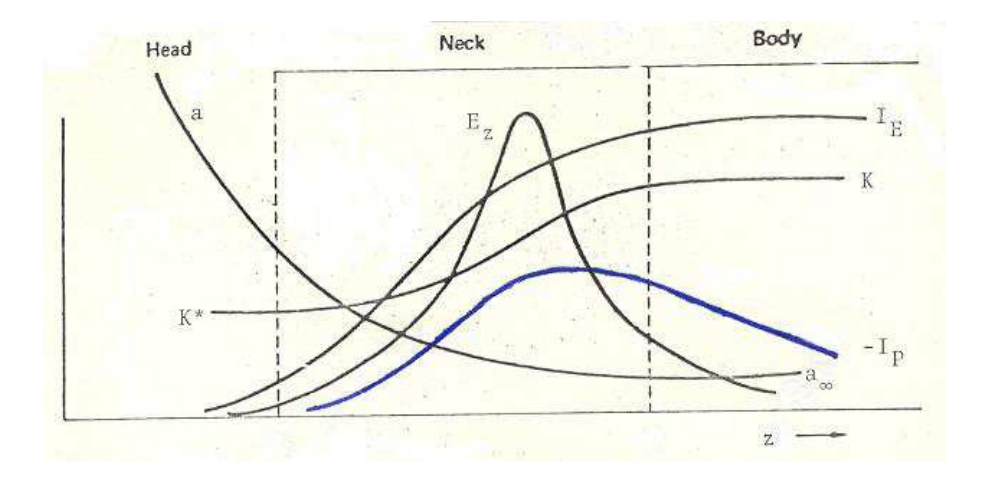


Figure 5.3: Beam neck profile. The variations of the effective beam current I_E , plasma return current I_P , kinetic energy K, longitudinal electric field E_z , and beam radius a, are shown in the neck region which separates the well-pinched body from the freely-expanding head of the beam pulse.

5.3 Beam head erosion and ohmic losses

In all situations, whether the beam is injected into a neutral gas or a plasma, the head of a pulse is not pinched and is followed by a neck in which there is a deep spike in the longitudinal electric field. The beam particles at the very front of the pulse will thus spread out radially and get lost, and those in the neck will lose energy because of the longitudinal electric field. As their energy decreases, the particles in the neck will also experience more scattering, and both effects will combine to increase the pinch radius. Consequently, the beam head expends continuously, and the neck region recesses progressively into the body of the pulse. (See Figure 5.3.)

This beam head erosion process has been studied both theoretically and experimentally [35, 41]. These studies show that after an initial transient period, the erosion process results in an almost constant rate of decrease in the length of the pulse as a function of the propagation distance.

The erosion rate can be estimated in a simple way by assuming that the particles in the neck will get lost when their kinetic energy has dropped from its initial value K down to some critical value K^* because of the ohmic losses in the longitudinal electric field. From (4.5) and (4.20), the erosion rate is thus

$$\frac{d\tau}{dz} = -\frac{q}{\pi\epsilon_0 c^2} \frac{d}{dK} (\mathcal{L}I_E) , \qquad (5.20)$$

which can be integrated to give the propagation range $z_{\delta t}$ corresponding to the decrease δt in the pulse duration:

$$z_{\delta t} = \pi \epsilon_0 c^2 \frac{K - K^*}{q \mathcal{L} I_E} \, \delta t \quad . \tag{5.21}$$

Assuming $K^* = K/2$ as suggested by experiments [35], this gives

$$z_{\delta t} = \frac{1}{8\mathcal{L}} \frac{K}{p} \frac{I_A}{I_E} \, \delta t \approx \frac{1}{8\mathcal{L}} \frac{I_A}{I_E} \, c \delta t \quad . \tag{5.22}$$

For a beam with K = 500 MeV, $I_E = 10$ kA, and $\mathcal{L} = 1$ at the neck, a beam pulse length loss of $\delta t = 10$ ns corresponds to a range of 600 m. Beam head erosion is thus a severe limitation to the propagation of short pulses.

Moreover, the estimate (5.20) has been obtained under the assumption that the particles in the beam neck do not move axially relative to the particles in the body of the pulse. This is a good approximation for electrons because in their case $\gamma^2 \gg 1$ at high energy. For protons, however, the condition $\gamma^2 \gg 1$ requires very large energies, of the order of several GeV, in order to be satisfied.

The ohmic losses are maximum in the head. However, for short pulses, the ohmic losses in the remainder of the pulse may also be important. From (4.7) and (4.20) one can calculate the range of a particle within a pulse subject to these losses:

$$z_{\Omega} = \frac{1}{4} \frac{K}{p} \frac{I_A}{I_P} \tau_m \approx \frac{c}{4} \frac{I_A}{I_B} \frac{\tau_m}{f_m} . \tag{5.23}$$

The maximum range is, of course, obtained for particles in the tail of the pulse where τ_m is maximum and f_m minimum.

The energy given up by ohmic losses primarily heats the plasma electrons. After the passage of the beam pulse, this energy contributes in forming a channel of hot air along the beam path. On the other hand, the energy lost in the form of radiations or particles scattered out of the beam do not contribute substantially into heating the air. The total energy deposited per unit length along the beam trajectory can be calculated by integrating the collision and ohmic terms in (4.20) over the length of the beam pulse:

$$\frac{\Delta W}{\Delta z} = \frac{I_B}{cq} \left(Sc\Delta t + 4cp\mathcal{L}\frac{I_E}{I_A} \right)$$
 (5.24)

where \mathcal{L} and I_E are evaluated at the end of the pulse.

Equation (5.24) shows that, for a high current beam, the energy depositions by ohmic losses can be larger than the energy deposition by collisions. This

happens when the gas pressure is low enough for collisions to be negligible, or when the pulse is short. Energy deposition can thus be enhanced by chopping a given pulse into a series of smaller pulses. If the individual pulses of the pulse train propagate independently from one another, they will, of course, all be subject to erosion. The most efficient configuration for energy deposition, for instance to bore a reduced density hole through the atmosphere in order to facilitate the propagation of subsequent pulses, will thus be a compromise.

Chapter 6

Stability of propagating high-power beams

6.1 General considerations on beam stability

A crucial question concerning beam propagation is that of stability. Because of the substantial source of free energy represented by the kinetic energy of the beam, a variety of instabilities could be excited and amplified during propagation. For the purpose of using high energy particle beams as weapons, the problem is to find a set of beam parameters (energy, current, radius, pulse length, emittance, and energy spread) such that the beam can reach the target without being destroyed by the possible instabilities. This is rather difficult, especially because the existing theoretical models predict stable beam propagation in such a narrow range of conflicting parameters that only the actual testing of a beam will confirm whether these predictions were correct or not.

The stability of beam-plasma systems is investigated by the standard perturbation method. If the initial perturbation of a stationary state of the system increases with time, the state is unstable under a perturbation of this type. Usually one seeks a solution of the system in the form

$$f(\vec{r},t) = f(\vec{r}) \exp i(\omega t - \vec{k} \cdot \vec{r})$$
(6.1)

where f is the deviation of any physical quantity from its stationary value. The relation between the complex frequency ω and the complex wave number \vec{k} is by definition the *dispersion relation*

$$D(\omega, \vec{k}) = 0 . ag{6.2}$$

A wave is said to be *unstable*, if for some real wave number k, a complex ω with a negative imaginary part is obtained from the dispersion relation, signifying growth in time of a spatially periodic disturbance:

$$\left. \begin{array}{l} \operatorname{Im}(k) = 0 \\ \operatorname{Im}(\omega) < 0 \end{array} \right\} \Longrightarrow \operatorname{Instability} .$$
(6.3)

The absolute value of the imaginary part of ω for an unstable wave $\delta = -\operatorname{Im}(\omega)$ is called the *increment* or *growth rate* (or its inverse the e-fold time) of the perturbation, because

$$f(\vec{r}, t) \propto \exp(\delta t)$$
 (6.4)

Instabilities in a beam-plasma system are primarily the result of the interaction between the beam and the plasma. The main parameters characterizing the plasma are its so-called *plasma frequency* (or *Langmuir frequency*) ω_p and ν the collision frequency of the plasma electrons. The plasma frequency is

$$\omega_p^2 = \frac{1}{\epsilon_0} \frac{e^2}{m_e} n_e \tag{6.5}$$

where n_e is the electron number density and m_e the electron mass. The plasma dielectric constant is then

$$\epsilon_p = 1 - \frac{\omega_p^2}{\omega(\omega + i\nu)} \ . \tag{6.6}$$

Similarly, as a plasma on its own, the beam is also characterized by its *beam* plasma-frequency (or beam Langmuir-frequency)

$$\omega_b^2 = \frac{1}{\epsilon_0} \frac{e^2}{m\gamma} n_b \tag{6.7}$$

where n_b is the beam particle number density, m the beam particles rest mass, and γ their Lorentz factor. The on-axis beam-plasma frequency is related to the beam scale radius by (4.2), and therefore

$$\omega_b^2 = 4 \frac{c^2}{a^2} \frac{I_B}{I_A} \ . \tag{6.8}$$

Finally, with the definition of the plasma frequency, the magnetic diffusion time (4.8) can be written

$$\tau_m = \frac{\omega_p^2 a^2}{\nu c^2} , \qquad (6.9)$$

and the charge neutralization time (4.3)

$$\tau_e = \frac{\nu}{\omega_p^2} \ . \tag{6.10}$$

There are numerous kinds of instabilities and many methods of classifying them. A rough phenomenological way is to divide them into two categories: macroscopic and microscopic. The next step is then to distinguish between various characteristics, such as the fate of the perturbation (absolute or convective), the driving forces (electrostatic, electromagnetic, etc.), the relative importance of collisions (collisional/non-collisional, resistive/ non-resistive), the relative importance of spread in the velocity distributions or temperatures (hydrodynamic, kinetic), etc. However, there is no sharp distinction between different possible categories. In this paragraph we will simply introduce the main concepts involved.

Macroscopic instabilities influence the spatial distribution of the beam. They are usually classified according to the geometry of the distorsion. For beams there are four main categories: (i) the *sausage* mode in which the beam contracts at regular intervals; (ii) the *hose* or *kink* mode in which the beam oscillates sideways; (iii) the *filamentation* mode in which the beam breaks up into several filaments; and (iv) the *ripple* mode in which the beam is distorted by small-scale ripples on the surface.¹

Macroinstabilities concern also other macroscopic degrees of freedom such as densities, hydrodynamic velocities, etc. They are connected with the flow-out of a plasma as a whole from one region into another. Macroscopic instabilities are also called *magnetohydrodynamic*, *hydrodynamic*, or simply *low frequency* instabilities.

Microscopic instabilities do not necessarily induce a macroscopic motion of the plasma as a whole, but they can excite local fluctuations of density and electromagnetic fields in the plasma. These *velocity-space* modes which do not appear to have direct effect on the beam will principally appear as an extra form of energy loss by which the energy of the beam can be transformed into powerful electromagnetic radiations. The most important kind of microinstability is the so-called *two-stream* instability. This mode is found when one is studying the propagation of electromagnetic waves in a system consisting of two interpenetrating streams of particles.

Some kinds of microinstabilities are directly connected to macroinstabilities. This is the case, for example, of filamentation which can be the macroscopic stage of a purely growing transverse electrostatic microinstability (the Weibel

¹This simple classification does not explicitly consider the *hollowing* modes, see Section 6.3.

instability). In general, the growth of microinstabilities may lead to the onset of macroinstabilities, which may eventually destroy the beam.

In a given reference frame, two types of instabilities can be distinguished physically: convective instabilities, and absolute or non-convective instabilities [43]. Briefly stated, the essential point is the distinction as to whether an initially localized disturbance (on an infinite system) grows exponentially with time locally (absolute instability) or ultimately decays because of the propagation of the growing disturbance away from the point of origin (convective instability). For a beam propagating along the z axis, the $group\ velocity$ of an unstable perturbation with longitudinal wave number k_z is given by

$$v_g = \frac{\partial}{\partial k_z} \operatorname{Re}(\omega) . \tag{6.11}$$

If v_g equals the beam velocity v, the perturbation is absolute in the beam frame; if $v_g = 0$, the perturbation is absolute in the plasma; and if $v_g < v$, the perturbation is convective. Clearly, for beam propagation, the worst instabilities are the absolute ones in the beam frame. Therefore, if an instability cannot be avoided, it should at least be convective in order not to completely hinder propagation.

The effect on stability of beam particle collisions with the plasma can, in general, be neglected except when, as with bremsstrahlung losses of high energy electron beams, they contribute to broadening the beam velocity distribution.

The collisions of the plasma electrons with the plasma molecules and ions often have an important effect on stability, and they can either increase or decrease the growth rates. When collisions are negligible, the instabilities are in the *collisionless* regime ($\nu \to 0$). In the *collisional* regime several distinctions can be made, in particular depending upon the relative values of the magnetic diffusion time τ_m and the collision frequency ν [44]. For high-current beams propagating in air, one has $\tau_m \nu < 1$ for pressures below a few Torr, and the instabilities are called *non-resistive*. For pressure above a few Torr $\tau_m \nu > 1$, and the instabilities are of the *resistive* kind. In the former case, the key parameter is the dielectric constant (6.6) and various time scale are possible for the growth rate. In the resistive case the time-scale is τ_m . When $\tau_e > \tau_m$, the acting forces are predominantly electrostatic, whereas, in the resistive domain where $\tau_m > \tau_e$, they are primarily magnetic.

In describing the electromagnetic oscillations associated with instabilities, especially in the case of microinstabilities, one often uses the standard conventions used for electromagnetic wave propagation in wave guides or plasmas. If \vec{E}_0 and \vec{B}_0 are the unperturbed fields, and \vec{E}_1 and \vec{B}_1 , their respective perturbations, one uses the following terminology:

- $\vec{B}_1 = 0$ electrostatic wave,
- $\vec{B}_1 \neq 0$ electromagnetic wave,
- $\vec{k} \parallel \vec{B}_0$ parallel wave,
- $\vec{k} \perp \vec{B_0}$ perpendicular wave,
- $\vec{k} \parallel \vec{E}_1$ longitudinal wave,
- $\vec{k} \perp \vec{E}_1$ transverse wave.

The hydrodynamic description of a beam-plasma system is strictly valid only in the limit of a monoenergetic beam penetrating a cold plasma. The velocity distribution of the beam (also called the *beam temperature*), and/or the velocity distributions of the plasma (the plasma ion and electron temperatures) can be taken into account by kinetic plasma theory. Neglecting the plasma temperature effects, the *hydrodynamic* regime of instability, as opposed to the *kinetic* regime, is defined by the following condition

$$|v_p - v| > \Delta v$$
 hydrodynamic regime $|v_p - v| < \Delta v$ kinetic regime (6.12)

where $v_p = \omega/k$ is the *phase velocity* of the wave, v the beam velocity, and Δv the RMS beam velocity spread. Introducing the *Doppler shifted wave frequency*

$$\Omega := \omega - \vec{k} \cdot \vec{v} , \qquad (6.13)$$

the kinetic regime is then defined as

$$|\Omega| < \vec{k} \cdot \Delta \vec{v} . \tag{6.14}$$

For self-pinched beams, the velocity distribution is the result of both the spread in beam energy (ΔW) and in beam direction (emittance). As $\tilde{v}_{\perp}^2 = \frac{1}{2}\tilde{v}_{\theta}^2$, where \tilde{v}_{θ} is the mean azimuthal velocity (4.14), the transverse and longitudinal components of the resulting velocity spread $\Delta \vec{v}$ are [45]

$$\frac{\Delta v_{\perp}}{v} = \sqrt{\frac{I_E}{2I_A}} = \tilde{\alpha} \quad , \tag{6.15}$$

$$\frac{\Delta v_{\parallel}}{v} = \frac{1}{2}\tilde{\alpha}^2 + \frac{1}{\gamma^2} \frac{\Delta W}{W} . \tag{6.16}$$

The combination of the effects of collisions with those of velocity spreads can considerably diminish the growth rate of instabilities. However, the most serious instabilities cannot completely be suppressed. Their effect will thus have to be minimized by the proper choice of beam parameters like current, shape, pulse length, deliberate velocity spreads, etc. In the following sections the major instabilities will be discussed together with possibles remedies.

6.2 Microinstabilities

When a beam passes at high velocity through a plasma, its coupling to the electrons or ions can excite unstable electromagnetic oscillations. For high energy beams propagating in ionized air, the coupling to the ions is in general negligible relative to to the coupling to the electrons. The resulting microinstabilities are of several different kinds depending upon the type of electromagnetic wave excited. The two most important ones are the so-called *two-stream instability*, which refers to transverse or longitudinal electrostatic waves, and the *Weibel instability* (or *micro-filamentation*) which is a transverse electromagnetic mode.

The complete analysis of the various types of streaming instabilities is rather complicated because the beam velocity distributions, the plasma temperatures, the beam's own magnetic field, etc., all have an effect on them. The theoretical analysis by analytical models is thus restricted to the most simple cases for which a linear perturbation approach is possible. The full analysis, including non-linear effects, requires computer simulations, and experiments will be needed to check the validity of the codes [23, 24]. The following discussion will present the main known results for the above-mentioned instabilities in the case of high energy beams launched into the air in the pressure range of interest for particle beam weapons.

6.2.1 Two-stream instability

The dispersion relation of the *two-stream instability* of a monoenergetic beam interacting with a cool plasma, neglecting the beam's own magnetic field, is [46]

$$1 - \frac{\omega_p^2}{\omega(\omega + i\nu)} - \frac{1}{\gamma^2} \frac{\omega_b^2}{\Omega^2} (\gamma^2 \sin^2 \phi + \cos^2 \phi) = 0$$
 (6.17)

where ϕ is the angle between the wave vector and the beam velocity, i.e.,

$$\vec{k} \cdot \vec{v} = kv \cos \phi = k_{\parallel} v \quad . \tag{6.18}$$

The unstable waves which are solutions to this dispersion relation are obtained by resolving it for ω and finding the roots which have a negative imaginary part. The peak growth occurs at $k_{\parallel}v = \omega_p$, and for $\nu > \omega_p$ it is given by

$$\delta = \operatorname{Im}(\omega) = \frac{\omega_b}{\gamma} \sqrt{\frac{\omega_p}{2\nu} (\gamma^2 \sin^2 \phi + \cos^2 \phi)} . \tag{6.19}$$

At relativistic energies, the fastest growing oscillations are those propagating almost perpendicular to the beam ($\sin\phi\approx 1$). Such an angular dependence is due to the fact that when $\gamma\gg 1$, the transverse mass $m\gamma$ of the beam particles is much smaller than the longitudinal mass $m\gamma^3$, and the oscillations which are transverse to the beam are easier to build up. The worst case will thus correspond to transverse waves for which

$$\delta \approx \omega_b \sqrt{\frac{\omega_p}{2\nu}} \sin \phi . {(6.20)}$$

The most difficult mode to suppress corresponds to $k_{\perp} = 1/a$ because the beam has finite radius a. Therefore

$$\sin \phi \approx k_{\perp}/k_{\parallel} = \frac{v}{a\omega_p} \ . \tag{6.21}$$

For air at atmospheric pressure, typical values for the plasma parameters of a 10 kA, 1 GeV, 0.5 cm radius electron beam are: $\omega_b = 5 \times 10^{10}$, $\omega_p = 6 \times 10^{12}$, and $\nu = 4.7 \times 10^{12} \, \mathrm{s}^{-1}$. Thus $\sin \phi = 0.01$ and the e-fold distance corresponding to the maximum growth (6.20) is $v/\delta \approx 1$ m, showing that two-stream instability ia a major obstacle to the propagation of monoenergetic beams over significant distances. However, taking the self-fields of the beam into account, the two-stream instability can be totally suppressed, provided the parameters fall into the kinetic regime.

The kinetic theory dispersion relation replacing (6.17) in the case of transverse waves takes the form [43]

$$1 - \frac{\omega_p^2}{\omega(\omega + i\nu)} - \omega_b^2 \int \frac{f(v)}{(\omega - kv)^2} dv \approx 0 .$$
 (6.22)

The integral over the beam velocity distribution f(v) has a singularity for $\omega = kv$, which was first studied by Landau for the collisionless damping of electromagnetic waves in warm plasmas (Landau damping effect). In the case of the two-stream instability, a similar effect is associated with the beam velocity distribution and results in the suppression of the instability [46]. This suppression becomes effective in the kinetic domain, which for two-stream instabilities sets in when

$$|\Omega| \approx \operatorname{Im}(\omega) < \vec{k} \cdot \Delta \vec{v}$$
 (6.23)

The transverse velocity spread due to particle oscillations in the pinch field is given by (6.15). The stability boundary, which is also the worst-case kinetic regime growth, is from (6.20) and (6.21)

$$\omega_b \sqrt{\frac{\omega_p}{2\nu}} < \frac{c}{a} \sqrt{\frac{I_E}{2I_A}} \quad , \tag{6.24}$$

which yields the condition [47]

$$\nu > \frac{2}{\omega_n} \frac{c^2}{a^2} \ .$$
 (6.25)

This simple stability criterion predicts that the two-stream instability will be suppressed for high-current high-energy beams propagating in air at pressures above a few Torr. This has been verified experimentally [48, 49] and has been confirmed by extensive computer calculations for beam energies up to 1 GeV and currents on the order of 10 to 100 kA [50].

Below the critical pressure implied by the collision frequency bound (6.25), the two-stream instability is not suppressed, but its growth rate is considerably reduced by kinetic effects. The growth rates of the longitudinal and transverse electrostatic waves, respectively, are then [45, 51]

$$\delta_{\parallel} = \frac{1}{2} \frac{1}{\gamma^2} \frac{\omega_b^2}{\omega_p^2} \nu \frac{v}{\Delta v_{\parallel}} , \qquad (6.26)$$

and

$$\delta_{\perp} = \frac{1}{2} \frac{\omega_b^2}{\omega_p^2} \nu \frac{v}{\Delta v_{\perp}} , \qquad (6.27)$$

and can be considerably lower than (6.20).

6.2.2 Weibel (or micro-filamentation) instability

The electromagnetic modes with \vec{k} normal to \vec{v} , \vec{E} nearly parallel to \vec{v} , and \vec{B} normal to both \vec{v} and \vec{E} , is a variety of the *Weibel instability*. This instability grows fastest in the absence of external or self-generated magnetic fields and is thus maximum for $f_m \approx 1$. It is an absolute instability which grows at perturbation centers of enhanced beam density which magnetically attract nearby beam particles and repel plasma electrons. Thus, the beam ultimately splits into filaments, each of which self-pinches. The computer simulations of this process [52] show that the filamentation stage in which the effect of this microinstability reaches the

macroscopic level, eventually ends up with the beam breaking up into separate filaments, which may recombine into a single dense beam, from which the return current is expelled.

For a charge- and current-neutralized beam, in which the self-fields are nearly suppressed, the dispersion relation of the Weibel instability for low frequencies $(\omega < \omega_p)$ is [52]

$$\omega^2 = -\beta^2 \frac{\omega_b^2}{1 + \frac{\omega_p^2}{k_1^2 c^2}} \tag{6.28}$$

where k_{\perp} is the transverse wave number. This is a purely growing mode and in the case of a collisional plasma it becomes [53]

$$\omega^3 = i\beta^2 \frac{\omega_b^2}{\omega_p^2} \nu k_\perp^2 c^2 \tag{6.29}$$

which shows that collisions enhance this kind of instability. In the kinetic regime, the growth of this instability is reduced, but kinetic effects alone are not sufficient to suppress it. This is because for such a transverse instability $|\Omega| < |\omega|$ and there is no such effect as Landau damping in that case.

The kinetic regime boundary (6.14) gives the maximum growth rate of this instability. Thus, from (6.29), it can be seen that

$$\delta = \frac{\omega_b^2}{\omega_p^2} \left(\frac{v}{\Delta v_\perp}\right)^2 , \qquad (6.30)$$

so that using (6.8) and (6.15) the maximum e-fold time in the kinetic regime is finally

$$\frac{1}{\delta} = \frac{1}{8} \tau_m (1 - f_m) . ag{6.31}$$

(When $f_m = 1$ the kinetic effects are absent and (6.29) applies.) The e-fold time (6.31) is very short and would, for this absolute instability, destroy the beam in few nanoseconds. However, this is only the case for $f_m \approx 1$ and a presence of a sufficient non-zero magnetic field results in the stabilization of this mode.

For collisionless plasmas, in the absence of an external magnetic field, the stability criterion is [54]

$$\left(\beta^2(1-f_m)-(1-f_e)\right) > \frac{1}{2} .$$
 (6.32)

This condition indicates that for a charge neutral beam ($f_e = 1$), a current neutralization fraction $f_m < 0.5$ provides enough self-magnetic field to stabilize the

micro-filamentation mode. For the case of collisional plasmas, there is no published analysis on the full effect of the self-fields. However, the criterion (6.32) is likely to still be applicable. This is, as is confirmed by the theoretical analysis [56], because this mode is always stable when the magnetic field B gives a beam particle cyclotron frequency $\Omega_c = qB/\gamma m$ larger than $\beta\omega_b$, which is true in our case since the self-magnetic field is equivalent to $\Omega_c = \sqrt{2}\beta\omega_b$ [54].

6.2.3 Discussion of microinstabilities

Concerning the stability of a beam with respect to microinstabilies, the situation can now be summarized as follows:

- At very low gas pressure, the plasma generated by the beam can be so week that the beam is only partially charge neutralized ($f_e < 1$), and the conductivity so low that $f_m \approx 0$. In that case, when $1 > f_e > 1/\gamma^2$, the beam is pinched but the plasma electron density may be insufficient for microinstabilities to develop. With electron beams, the two-stream instability is avoided as long as the product of gas pressure and pulse length is low enough to keep secondary electrons from accumulating inside the beam [55]. This is sometimes referred to as the *low pressure propagation window*, in which the beam propagates in the so-called *ion-focused regime* (IFR). For air, it corresponds to about 10^{-6} Torr for a 10 kA beam [22, 55]. For such a beam, with an energy of 500 MeV, the range would be on the order of 200 km [55].
- At intermediate pressures, the two-stream mode sets in, and the beam becomes unstable. The range of the beams is then determined by the maximum growth rate given by (6.26) or (6.27).
- At pressures above a few Torr, for beam currents in the 10 to 100 kA range, the two-stream instability is suppressed. This has been observed in many experiments for a review see [12] and for actual experiments [23, 48]. However, above the critical pressure, the rise in plasma conductivity enables a return current to flow and filamentation becomes possible as f_m → 1. Moreover, because of this increase in conductivity, other new instabilities, including macroinstabilities, also become possible. Therefore, the narrow stability window observed in air near 1 Torr is due to the suppression of microinstabilities by collisions and kinetic effects, and to the temporary absence of resistive macroinstabilities which set in at higher pressures.

6.3 Macroinstabilities

The small amplitude distorsion of the shape of a cylindrical beam can be described by giving the perturbed form of the beam surface:

$$r = a + \Delta r(z, r, \theta, t) . \tag{6.33}$$

The standard method is to make a multipole expansion of the perturbation in a thin annulus as a function of the azimuthal angle θ

$$\Delta r = \sum_{m} \Delta r_m(z, r, t) \cos m\theta . \qquad (6.34)$$

For small amplitude periodic perturbations, this can be Fourier analysed as a superposition of modes such that [57]

$$\Delta r = \sum_{m} A_m(r) \exp i(\vec{k} \cdot \vec{r} - \omega t + m\theta) . \qquad (6.35)$$

The mode m=0 displays harmonic variations of beam radius with distance along the beam axis: this is sausage instability. The mode m=1 represents transverse displacements of the beam cross-section without change in the form or in a beam characteristics other than the position of its center of mass: this is called sinuous, kink or hose instability. Higher values of m represent changes of cross-section from circular form: m=2 gives an elliptic cross-section, m=3 a pyriform cross-section, etc. Modes with m>1 are referred to as filamentation modes, because their growth leads towards the break-up of the beam into separate filaments.

For a given azimuthal wave number m, various radial modes are possible. They are usually classified according to the degree 2n of polynomial eigenfunctions of the dispersion equation. For example, when m=0, n=0 corresponds to axial hollowing, n=1 to standard sausaging, n=2 to axial bunching, etc., [58]. A systematic classification of the modes excited by resistive macroinstabilities in a simplified helical orbit beam model has been given by Steven Weinberg [59].

The primary concern with macroinstabilities is to determine their growth rate and the conditions for which they are sufficiently convective to ensure that the growth will be of limited consequence for a sufficiently short beam pulse. The analysis is then simpler in the Doppler-shifted frequency representation of the oscillations:

$$\exp i(kz - \omega t) := \exp i(\Omega z/v - \omega \tau) . \tag{6.36}$$

In this representation, τ gives the position of a section of the beam pulse measured from the head of the beam (5.1), and Ω is the Doppler-shifted frequency (6.13).

When Ω is real, and ω complex, the dispersion relation $D(\Omega, \omega) = 0$ yields solutions giving the free growth of instabilities corresponding to initial value problems in the beam frame. These are potential instabilities developing during the flight of the beam towards its target. It is thus crucial that these instabilities are convective, i.e., that $\operatorname{Re} \omega(\Omega) \neq 0$.

When ω is real, and Ω complex, the same dispersion relation yields solutions to initial value problems in the accelerator frame. The convective nature of these instabilities, or the limited duration for the acceleration period for absolute instabilities, will ensure that their effect will disappear after the pulse has left the accelerator. For practical reasons, one usually studys macroinstabilities in laboratory experiments by deliberately introducing perturbations at the end of the acceleration process [60]. In the following discussion, we will assume that the accelerator can be built in such a way that the pulse is not disturbed during acceleration. We will thus concentrate on instabilities affecting the flight of the beam towards its target.

6.3.1 Electrostatic kink instability

Analysis of the major macroinstabilities for propagation in air at pressure between 0.01 and 1 atmosphere shows that only short pulses may propagate over sizable distances. Furthermore, because of the considerable difference in relativistic mass between transverse and longitudinal motions of the beam, instabilities involving transverse displacement wil grow fastest. As a result, the first order description of a beam pulse during the early stages of the growth of an instability, will not be that of a thin and flexible thread but of an axially rigid rod, the cross-section of which is undergoing distorsion. This is the so-called *rigid beam* approach.

However, in the case of a beam propagating in a vacuum or a low density plasma, the *thin thread* approximation can be satisfactory. Let us consider, for example, the stability of a charged beam in a vacuum, and then the effects of a plasma on it [61]. In that case, the most serious instability is the m=1 electromagnetic kink mode in which the beam is distorted as a flat snake or a screw. The growth rate can be determined by analysing the lateral motion of a flexible cylinder of charged particles in a vacuum. The calculation is easiest in the beam frame, and after Lorentz transformation into the accelerator frame the result is

$$\Omega = -\frac{1}{2}i\omega_b \frac{ka}{\gamma} \sqrt{\ln(\frac{ka}{\gamma})} . {(6.37)}$$

Because of the finite radius of the beam, the growth rate $\delta = -\operatorname{Im}(\omega) = -\operatorname{Im}(\Omega)$

for $k=k_{\parallel}$ real, has a maximum at $ka=0.6\gamma$, and a cut-off at $ka=\gamma$. In the rest frame of the beam, the effect of a plasma environment is to reduce the electric field by a factor equal to the dielectric constant (6.6): hence to reduce the growth rate by $1/\sqrt{\epsilon_p}$. When $\nu>kv$, (6.37) then becomes

$$\Omega = -\frac{1}{2}i\frac{\omega_b}{\omega_p}\frac{ka}{\gamma}\sqrt{\frac{1}{2}\nu kv\ln(\frac{\gamma}{ka})} . \tag{6.38}$$

This is the dispersion relation of the electrostatic kink instability in the hydrodynamic limit for a thin beam. It applies for beams propagating in collisional plasmas under such conditions that the magnetic forces can be neglected. This is the case in air at pressures below 1 Torr. The maximum growth rate is at $ka=0.72\gamma$:

$$\delta = \frac{1}{4} \sqrt{\frac{\gamma}{\tau_m}} \frac{v I_B}{a I_A} \ . \tag{6.39}$$

In the kinetic regime, this instability is damped when ${\rm Im}(\Omega) < k \Delta v_{\parallel}$. This happens when

$$\tau_m > \frac{2}{\gamma} \frac{a}{v} \frac{I_A}{I_B} \ . \tag{6.40}$$

Let us consider now the stability problem of a rigid beam subject to transverse displacements. This is the m=1 mode, and it is easiest to start by considering first a beam with a constant density profile and a sharp boundary, even though we will have to examine later the more realistic case of a beam with the Bennett profile. We further assume that the beam is fully charge neutralized by a collisional plasma of constant density with radius larger than the beams radius.

If a beam is slightly displaced in the transverse direction, a surface charge density distribution with a $\cos\theta$ azimuthal dependence will appear. Such a charge distribution produces a homogeneous dipolar electric field which results in an electrostatic restoring force directly proportional to the displacement. For a beam with a flat density profile, the equation of motion is simply [62]

$$\frac{d^2}{dt^2}y_b = -\frac{1}{2}\omega_b^2(y_b - y_p) , \qquad (6.41)$$

where y_b is the position of the axis of the displaced beam, y_p the position of the axis of the non-neutral plasma column which neutralizes the beam, and $\frac{d}{dt} = \frac{\partial}{\partial t} + v \frac{\partial}{\partial z}$ the total derivative. From the equation of continuity and Gauss's law one can see that the plasma will move according to

$$\frac{\partial}{\partial t}y_p = \frac{1}{\tau_e}(y_b - y_p) . {(6.42)}$$

Taking small perturbations of the form $\exp i(kz - \omega t)$, this couple of equation yields the dispersion relation

$$-i\omega\tau_e = \frac{\Omega^2}{\frac{1}{2}\omega_b^2 - \Omega^2} \ . \tag{6.43}$$

This is the electrostatic kink instability. For Ω real, ω is purely imaginary and the growth is absolute in the beam frame. Furthermore, the growth rate $\delta = -i\omega$ tends to infinity as Ω^2 approaches $\frac{1}{2}\omega_b^2$. If we take for τ_e the complete expression

$$\tau_e = \frac{\nu - i\omega}{\omega_p^2} \tag{6.44}$$

the dispersion relation (6.44) can be put in the more familiar form [63]

$$\frac{\omega_e^2}{\omega(\omega + i\nu)} + \frac{1}{2}\frac{\omega_b^2}{\Omega^2} = 1 \quad . \tag{6.45}$$

Apart from the factor $\frac{1}{2}$, it is identical to the dispersion relation for transverse (i.e., $\phi = \frac{\pi}{2}$) two-stream instability (6.17). In the collisionless limit ($\nu = 0$) this result is well known to particle accelerators specialists [62].

6.3.2 Electromagnetic kink (or "resistive hose") instability

In a low conductivity plasma, τ_e is very large and (6.43) reduces to stable oscillations at frequency $\Omega^2 = \frac{1}{2}\omega_b^2$. Physically, this corresponds to a beam neutralized by infinitely heavy ions, so that the beam's motion is simply harmonic oscillations about a cylinder of neutralizing charges which cannot move. This is obvious from (6.42) which shows that y_p is constant when $\tau_e = \infty$. At the other limit of high conductivity τ_e becomes very small. In that case (6.42) indicates that $y_b = y_p$, and this corresponds to the fact that when conductivity is very high the plasma neutralizing the beam can follow it exactly, and there are no electrostatic beam oscillations or instabilities. However, when the conductivity is high, magnetic forces have to be taken into account:

When a beam is displaced transversely to its direction of propagation, the motion of the magnetic field generated by the beam current J_B induces a longitudinal electric field. If $\vec{v}_y = \frac{\partial}{\partial t} \vec{y}_b$ is the velocity of the sideways beam displacement and \vec{B}_θ the azimuthal magnetic field, the Lorentz transformation of this magnetic field gives $\vec{E}_z = \vec{v}_y \times \vec{B}_\theta$ in the limit of small \vec{v}_y . This electric field generates a longitudinal plasma current $\vec{J}_z = \sigma \vec{E}_z$, which, if the plasma conductivity is high enough, generates an azimuthal magnetic field of sufficient strength to interfere

with the beam-current-generated azimuthal magnetic field. (This plasma current should not be confused with the plasma return current, which we assume to be negligible for the moment, $f_m=0$.) As the displacement of the plasma does not coincide with that of the beam when the conductivity is finite, the total magnetic field resulting from J_B and J_z will have an axis y_m different from the beam axis y_b or the plasma current axis y_p . This displacement of that magnetic field axis is directly related to the magnetic diffusion time. Thus

$$\frac{\partial}{\partial t}y_m = \frac{1}{\mathcal{L}\tau_m}(y_b - y_p) . agen{6.46}$$

When the conductivity is low (i.e., τ_m small) the plasma induced by the lateral displacement is negligible and $y_m = y_b$, i.e., the magnetic axis always corresponds to the beam axis. On the contrary, when the conductivity is high (i.e., τ_m large), or the plasma infinite in extent (i.e., $\mathcal{L} \to \infty$), y_m is constant and the magnetic field is "frozen." When the magnetic field axis does not correspond with the beam axis, the particles in the beam are subjected to a restoring magnetic force which is equivalent to the force needed to drive the plasma current J_z . This force can be determined from the effect on the beam of the dipolar magnetic field resulting from the differences in position between the beam and the magnetic field axis. This gives

$$\frac{d^2}{dt^2}y_b = -\frac{1}{2}\beta^2\omega_b^2(y_b - y_m) . {(6.47)}$$

For periodic small amplitude oscillations, the system (6.46), (6.47) gives the following dispersion relation [64, 65]

$$-i\omega \mathcal{L}\tau_m = \frac{\Omega^2}{\frac{1}{2}\beta^2\omega_b^2 - \Omega^2} . \tag{6.48}$$

This is the dispersion equation of the *electromagnetic kink* or *hose instability* of a rigid beam in a resistive plasma. It shows absolute instability in the beam frame and infinite growth for $\Omega^2 \to \frac{1}{2}\beta^2\omega_b^2$. This resistive hose instability has been extensively studied [58], [59], and [64] to [70].

The dispersion relation (6.48) is similar to its electrostatic counter part (6.43), but corresponds to a different driving mechanism. In fact, for $\tau_m < \tau_e$, the kink instability is of the electric kind and the dispersion relation is (6.43). On the other hand, in high conductivity plasmas $\tau_m > \tau_e$ and the instability is of the magnetic kind, and the dispersion relation is (6.48). In the limit of $\tau_m \approx \sigma = 0$, the electric oscillations are stable with frequency $\Omega^2 = \frac{1}{2}\omega_b^2$, and in the limit $\tau_m \approx \sigma = \infty$, the magnetic oscillations are stable with frequency $\Omega^2 = \frac{1}{2}\beta^2\omega_b^2$.

6.3.3 Macrostability of a beam penetrating a neutral gas

In the case of a beam penetrating a neutral gas and generating it own plasma, the electric and magnetic kink modes are encountered successively as the conductivity rises from zero to a maximum. A model valid for arbitrary conductivity and combining the two instabilities is thus important. Such a model is obtained by combining (6.41), (6.42), (6.46), and (6.47). This leads to the system of equations:

$$\frac{d^2}{dt^2}y_b + \frac{1}{2}\omega_b^2(y_b - y_p) + \frac{1}{2}\beta^2\omega_b^2(y_b - y_m) = 0 , \qquad (6.49)$$

$$\frac{\partial}{\partial t}y_p + \frac{1}{\tau_e}(y_p - y_b) = 0 , \qquad (6.50)$$

$$\frac{\partial}{\partial t}y_m + \frac{1}{\mathcal{L}\tau_m}(y_m - y_b) = 0 . ag{6.51}$$

The resulting dispersion relation is [58, 70]

$$(1 - i\omega \mathcal{L}\tau_m)(1 - i\omega\tau_e) = \frac{\frac{1}{2}\omega_b^2(\beta^2 + i\omega\tau_e\gamma^{-2} + \omega^2\tau_e\mathcal{L}\tau_m)}{\frac{1}{2}\beta^2\omega_b^2 - \Omega^2} .$$
 (6.52)

As the m=1 oscillations are stable in the limits $\sigma=0$ and $\sigma=\infty$, the instability growth rate has a maximum at some finite value of the conductivity. The dispersion relation (6.52) shows that this maximum is obtained when

$$\tau_e = \mathcal{L}\tau_m = \frac{a}{c}\sqrt{\mathcal{L}} . {(6.53)}$$

By comparison with (5.9) and (5.12), one sees that this happens at a point very early in the beam pulse, and that m=1 instabilities will have maximum growth in the neck region.

In the head region of the beam, τ_m and τ_e are directly function of the beam current (5.9). Therefore, in order to minimize the length of the neck region over which the growth is largest, the conductivity generation by the beam should be as large as possible, requiring

$$I_B > I_G$$
 . (6.54)

However, this condition implies high plasma return currents: the hose instability should therefore be examined in the $f_m \neq 0$ case as well.

A non-zero plasma return current has essentially no effect on the electrostatic forces, and thus on the electric kink instability. On the other hand, the magnetic forces are directly affected, and the first effect of a return current is to diminish the

magnetic force in (6.47) by the factor $(1-f_m)$ which is equivalent to replacing by I_E the current I_B used to calculate ω_b^2 with (6.8). But there is also an additional effect: as anti-parallel currents tend to repel each other, when the beam is displaced relative to the plasma channel in which the return current flows, the interaction between the beam current and the return current tends to increase the displacement. This is the so-called *self-hose* effect which results in a supplementary force on the beam proportional to $I_BI_P=f_mI_B^2$. Including those two effects, the equation of motion (6.47) becomes

$$\frac{d^2}{dt^2}y_b = -\frac{1}{2}\beta^2\omega_b^2(y_b - y_m)(1 - f_m) + \frac{1}{2}\beta^2\omega_b^2y_mf_m$$

$$= -\frac{1}{2}\beta^2\omega_b^2(y_b(1 - f_m) - y_m) .$$
(6.55)

Similarly, they results into the replacement of ω_b^2 by $\omega_b^2(1-f_m)$ in the denominator on the right hand side of equation (6.52), [58]. Thus, for $\tau_m > \tau_e$,

$$-i\omega \mathcal{L}\tau_m = \frac{\frac{1}{2}\beta^2 \omega_b^2 f_m + \Omega^2}{\frac{1}{2}\beta^2 \omega_b^2 (1 - f_m) - \Omega^2} .$$
 (6.56)

With the effect of the self-hose included, the growth rate of the magnetic hose instability is clearly worse. In particular contrary to (6.48), the growth rate at $\Omega=0$ is now non-zero. This implies that when $f_m\neq 0$, even a very slow transverse displacement may result in the disruption of the beam. Furthermore, as $f_m\to 1$, the growth rate increases and the position of the pole moves towards smaller frequencies.

The electric and magnetic hose modes for rigid oscillations of flat profile cylindrical beams show very bad stability properties. The consequences of various damping effects on these instabilities will be discussed below. Before that, we will examine the $m \neq 1$ modes with the same flat profile rigid beam model, but only for resistive modes in the limit of $\tau_m > \tau_e$.

For m=0, the sausage mode dispersion relation is as follows [58, 71]

$$-i\omega \frac{1}{6}\tau_m = \frac{-\beta^2 \omega_b^2 (1 - 2f_m) + \Omega^2}{2\beta^2 \omega_b^2 (1 - f_m) - \Omega^2} . \tag{6.57}$$

The main difference between this dispersion relation and the hose dispersion relation (6.56) is that the sausage mode is unstable in a limited frequency range only: for $f_m \approx 0$, between ω_b and $2\omega_b$. This will enable the kinetic effects to stabilize this instability provided that, as can be seen from (6.57),

$$f_m < \frac{1}{2}$$
 (6.58)

For m > 1, there are numerous unstable modes possible. However, in the limit of small f_m , the main modes obey the approximate dispertion relation [59]

$$-i\omega\tau_m = \frac{-(m^2 - 1)\frac{1}{2}\beta^2\omega_b^2 + \Omega^2}{m^2\frac{1}{2}\beta^2\omega_b^2 - \Omega^2} . {(6.59)}$$

In the case m=1 one recognizes the hose mode, and for m>1, similarly to the sausage mode, instabilities exist only in a limited frequency range, which becomes narrower in proportion when m^2 increases.

The essential difference between the hose mode and the $m \neq 1$ modes is that when m=1 a low frequency disturbance can be produced without internal compression or distorsion: only a simple transverse displacement is required [59, 65]. Because there is no change in internal pressure to produce a restoring force, hose instability appears at an arbitrary low (Doppler shifted) frequency. Furthermore, the stabilizing effects of possible spreads in the beam velocities vanish in that limit. For the $m \neq 1$ modes, instability potentially appears at finite frequency, but is strongly suppressed by kinetic effects. We will thus concentrate on these effects on the hose mode only, assuming that coping with this worst case mode will be sufficient.

6.3.4 Macrostability of beams with rounded radial profiles

In examining now the stability of more realistic beam plasma models we will see that the instabilities are somehow not so bad as for idealized models such as the sharp boundary, flat profile, cylindrical beam studied so far. We will first look at the effect of rounded beam profiles — specifically of the Bennett profile (4.16) — and then at the effect of spreads in velocity distribution, mainly arising from the particle's oscillations in the pinch field.

Let us rewrite the hose dispersion relation for $f_m = 0$ in the following form

$$-i\omega\tau_b = \frac{\Omega^2}{\beta^2\omega_\beta^2 - \Omega^2} \ . \tag{6.60}$$

 ω_{β} is the *betatron frequency*, equation (4.15), which for a beam with a flat current profile is simply

$$\omega_{\beta}^2 = \frac{1}{2}\beta^2 \omega_b^2 := \omega_{\beta m}^2 \ . \tag{6.61}$$

In the case of a beam with the Bennett profile (4.16), the betatron frequency is not constant but uniformly distributed between zero and the maximum $\omega_{\beta m}$. The

force equation (6.47) has then to be averaged over the Bennett distribution and the resulting effective betatron frequency is [65]

$$\omega_{\beta}^2 = \frac{1}{6}\beta^2 \omega_b^2 \quad . \tag{6.62}$$

Similarly, for the magnetic axis diffusion equation (6.46), the dipole magnetic diffusion time must be recalculated by properly averaging over the beam and plasma conductivity profiles. Assuming the beam current and the plasma conductivity to both have Bennett profiles with scale radius a for the beam and b for the plasma, one finds

$$\tau_d = \frac{3}{2} \frac{\eta^4}{(\eta^2 - 1)^2} \left(\frac{\eta^2 + 1}{\eta^2 - 1} \log(\eta) - 1 \right) \tau_m \tag{6.63}$$

where $\eta = b/a$. In the case where a = b, this is

$$\tau_d = \frac{1}{8}\tau_m \quad , \tag{6.64}$$

and by comparison with (6.63) one sees that $\tau_d > \frac{1}{8}\tau_m$ when b > a, so that the beam is more stable in the case where the conductivity profile is broader than the beam profile [69].

The dispersion relation (6.60) has been derived in the hydrodynamic limit. However, from (6.60) and (6.15),

$$|\Omega| = \omega_{\beta} \frac{|\omega|\tau}{\sqrt{1 + |\omega|^2 \tau^2}} < k_{min} \Delta v_{\perp} = \omega_{\beta} . \tag{6.65}$$

Thus, according to (6.14), kinetic effects cannot be ignored for the hose instability. The simple dispersion relation (6.60) should therefore be replaced by the expression

$$-i\omega\tau_d = \int_0^{\omega_{\beta m}^2} f(\omega_\beta^2) \frac{\Omega^2}{\beta^2 \omega_\beta^2 - \Omega^2} d\omega_\beta^2$$
 (6.66)

where $f(\omega_{\beta}^2)$ is a suitable distribution function. In principle this distribution function could be derived from the Vlasov kinetic plasma theory. But an exact solution to this problem has still not been found. However, two different phenomenological approaches [65, 66], which agree with computer simulations [69], give plausible results with the following function

$$f(\omega_{\beta}^2) = 6 \frac{\omega_{\beta}^2}{\omega_{\beta m}^2} \left(1 - \frac{\omega_{\beta}^2}{\omega_{\beta m}^2} \right) . \tag{6.67}$$

For $f_m = 0$, the resulting dispersion relation is [65, 66]

$$-i\omega\tau_d = 6\frac{\omega_\beta^2}{\omega_{\beta m}^2} \left(\frac{1}{2} - \frac{\Omega^2}{\omega_{\beta m}^2} + \frac{\Omega^2(\omega_{\beta m}^2 - \Omega^2)}{\omega_{\beta m}^4} \log \frac{\omega_{\beta m}^2 - \Omega^2}{\Omega^2}\right) . \tag{6.68}$$

In comparison with (6.60), this dispersion relation shows much less serious instability problems:

• The growth rate has a cut-off at $\Omega = \omega_{\beta m}$ and there is no pole at $\Omega = \omega_{\beta}$. Instead, for $\Omega = 0.52 \omega_{\beta m}$, the growth rate has a maximum

$$\delta_{max} = \frac{0.69}{\tau_d} \ . \tag{6.69}$$

• The instability, from absolute in the beam frame, becomes convective. Therefore, as a perturbation of the beam grows, it will at the same time move backwards into the pulse. For a perturbation of amplitude y(0) generated at the head of the beam, a saddle point analysis of the dispersion relation [65] shows that the growth of the hose is such that at the tail of the beam pulse its amplitude will be

$$y(\Delta t) = y(0)\left(1 + \frac{\Delta t}{\tau_d}\right) . (6.70)$$

The existence of a maximum and of a cut-off in (6.68) have been verified experimentally [60]. Similarly, other experiments [48] have also demonstrated the convective nature of the hose instability. In these experiments, the hose instability leads to an erosion of the beam tail. This is because, for a beam of finite duration, the disturbance is maximum at the end of the pulse.

The significance of (6.70) is that for a pulse of finite duration, a disturbance ultimately disappears. Thus, if a beam pulse has a duration of the order of τ_d , it will be able to propagate over large distances. In practice, the problem is that τ_d is only of a few nanoseconds for a high current beam injected into the atmosphere at normal pressures. Therefore, stable beam propagation is restricted to very short pulses.

A further difficulty with the hose instability is that its maximum growth and its convective nature depend on the extent of current neutralization of the beam. It is found, for instance, that even a small amount of current neutralization (i.e., $f_m \approx 0.1$) is strongly destabilizing, particularly at low frequencies, and leads to absolute instability as seen by the beam [66]. The hose instability in the presence of current neutralization has been studied on a computer in the frame work of the Vlasov theory [69]. The results show that for a current neutralization fraction larger than 0.5 the return current driven self-hose becomes the dominant destabilizing mechanism.

The general properties of the hose instability can be transposed to the case of the $m \neq 1$ macroinstabilities and this has been verified in a number of cases. For example, it has been found that the sausage mode is stable provided that [69]

$$\frac{f_m}{1 - f_m} < 2\frac{I_B}{I_G} \ . \tag{6.71}$$

Similarly, general considerations show that filamentation can be avoided if [72]

$$\frac{\tau_m}{\Delta t}(1 - f_m) = 1 \quad . \tag{6.72}$$

6.3.5 Discussion of macroinstabilities

In conclusion, the stability with respect to macroinstabilities seems to be ensured for beams of pulse length of the order of τ_m , provided that f_m is small. In practical cases, these requirements may be somewhat less stringent. For instance, the effect of various damping factors (such as variations of beam current during the pulse, energy spreads, smooth radial and longitudinal beam profiles, finite pulse length, etc [22]) cannot be calculated easily. Experiments such as those that are possible with the high-current high-energy accelerators which have been proposed or built at Los Alamos [23], Livermore, [24] and in the Soviet Union [73] are thus crucial.

Finally, because of the need for short pulses, actual beam weapon systems will have to use trains of small pulses in order to send sufficient energy towards the target. This creates various problems, because pulses within a train will have to propagate in the plasma background generated by the previous pulses. The analysis of these problems, together with that of the boring of reduced density plasma channels, will be part of the conceptual design of practical particle beam weapons.

Chapter 7

Discussion of theoretical prospect

We have examined the main physical problems involved in the propagation of particle beams for possible exo-atmospheric or endo-atmospheric beam weapon systems.

There is no problem of principle with the propagation of neutral particle beams in outer space. Systems with adequate characteristics are under development since more than twenty years [10]. For short range exo-atmospheric systems, i.e., on the order of a few hundreds of kilometers, charged beams or plasmoîd beams might eventually be used.

For land-based systems, the main problem is to cope with the conflicting nature of the following set of conditions:

- 1. The beam power has to be larger than the Nordsieck power (4.24) in order for the beam to propagate over sizable distances;
- 2. the beam current should be less than the critical current (5.8), and the current neutralization fraction as small as possible (5.15), so that the beam is well pinched;
- 3. the beam pulses have to be long enough so that they will not be completely eroded before reaching their target (5.22). Furthermore, the beam should be relativistic enough ($\gamma > 10$) for the steady state erosion hypothesis to be valid;
- 4. the pulse duration has to be of the order of the dipole magnetic diffusion time so that propagation is not disrupted by macroinstabilities (6.70);

- 5. in order to keep the growth of instabilities at a minimum, the current neutralization should be minimized (6.32), (6.56), (6.58), (6.71), and (6.72), and the conductivity should rise fast enough to avoid excessive growth in the head (6.54);
- 6. the beam radius, emittance, energy, and current should match the Bennett pinch radius (4.12) at the exit of the accelerator system, and should be compatible with the requirements of beam stability and hole boring.

These conditions cannot easily be simultaneously satisfied. This is primarily because the pulse length is set by magnetic diffusion time. For a given beam radius, this time can only be increased by increasing the beam current, and thus producing an undesirable large current-neutralization fraction.

However, within rather tight limits, a set of acceptable beam parameters seems to exist. In order to find out if these conditions are really satisfactory for beam weapon applications, careful experiments are needed. This concluding sentence was written in November 1982, together with the additional remark: These crucial experiments will be done with accelerators currently under construction in the United States [23, 24] and probably in the USSR [73]. Within a couple of years, at most, the final answer should be known. What can we add to this conclusion, more then twenty years after it was written?

- First: That the laws of physics have not changed, and that the theoretical analysis done in the previous chapters remains valid. In fact, having followed the literature over the past twenty years, it appears that nothing really new and important has been found and published. In particular, the most difficult theoretical problems addressed in this report the questions related to the stability of propagating a charged-particle beam through a pre-existing or beam-generated plasma are still discussed in recent papers by referring to the seminal work done during the 1960s to the 1980s. This is not to say that no progress has been made, but that the basic physical processes at work in high-intensity high-energy beam propagation in plasmas appear to have been properly recognized and analysed during these decades.
- Second: That a major step in the theoretical understanding of beam-propagation stability was made between the time of the early analytical calculations, such a those of Steven Weinberg [59], and the time of the more sophisticated studies, such as those of Edward P. Lee [65], which showed that

¹See, for example, references number 20 to 25 cited in a recent paper where the resistive hose instability is reinvestigated for low-collisional plasmas [77].

oversimplified models were likely to predict far too pessimistic behaviors in comparison to more realistic ones. This means that an essential step after accelerating a beam pulse is that of "conditioning," that is of shaping and smoothing its spatial an possibly temporal extent in such a way to avoid the onset and growth of instabilities during propagation.²

- Third: That some experimentally well-established observations, such as stable long-distance propagation in low-density gas (i.e., in the ion-focused regime [55]), are now also much better understood theoretically than some years ago [74]. This means that one can have much greater confidence in the theory, both for free-propagation in high- or low-density air, as for controlled transport and conditioning in the accelerator system generating the beam. In particular, the interaction of intense relativistic electron beams with preformed laser-generated channels in the atmosphere [75], as well as the stability of such beams in beam-induced channels [76], appear to confirm present understanding of such phenomena.
- Fourth: That technological advances are constantly changing the context in which specific systems have to be assessed, both from a theoretical then from an experimental point of view [78]. For example, the possibility of the use of antihydrogen beams in exo-atmospheric systems came to the author's mind in 1983 when a former CERN colleague told him about Los Alamos management's interest to hire him for antimatter work at their laboratory [79]. This lead him to realize that antimatter was the sole portable source of muons, which are the main byproducts of the annihilation of antiprotons with matter [80]. This means that if muons from such a source could be "cooled"³ and accelerated, the possibility of exploiting the high-range of muon beams (see Figures 4.2 and 4.3) would become theoretically possible. In fact, as will be seen in Section 10.5, the problem of generating and cooling intense beams of muons is the subject of vigorous research since a few years. While this effort may not succeed in producing muon-beams sufficiently intense to propagate in self-pinched mode over significant distances, the development of muon technology for fundamental research will help assessing whether muon beams, and beams of their related neutrino decay products, may have other practical applications [81, 82].

²This is the plasma-physical counterpart of the hydrodynamical need to smooth boundaries and remove all unwanted discontinuities in order to avoid drag, turbulence, and instabilities in the motion of ships, aircrafts, or missiles.

³"Cooling" means decreasing the kinetic energy dispersion of a bunch of particles.

Chapter 8

Discussion of beam propagation experiments

The discussion of the experimental prospect of particle beam technology for exoatmospheric applications is quite different from that of endo-atmospheric applications.¹ Indeed:

• Exo-atmospheric beam technology is very similar to the relatively lowintensity (mA), relatively high-energy (GeV), beam technology used in numerous, officially non-military, national and international nuclear and elementary-particle research laboratories. Moreover, the typical accelerator and beam steering technologies required for outer-space beam weapons is very similar to those of emerging applications of accelerators such as cancer therapy, breeding of fissile and fusion materials, transmutation of nuclear waste, breeding of antimatter [84], or proton-radiography of the detonation of conventional explosives and nuclear weapon's primaries, [85] and [86, p.84–89]. Finally, the more advanced technology for beam weapons is significantly overlapping with that of next-generation research accelerators such as the Large hadron Collider (LHC) at CERN and the future linearcollider to be built (most probably in the US) as a fully international effort [87]. This means that most components of space-based beam weapons can be developed and tested in civilian laboratories (Section 9.1), and that the role of military laboratories is to develop and test systems which integrate these components, and merge them together with the application specific

¹A summary of the early efforts on particle beam weapons research, from World War II to 1980, as well as some comments on Soviet particle beam research, are given in a comprehensive fact-sheet published by the U.S. Department of Defense [83].

technologies related to their use in an outer-space battle-field environment, rather than as research tools in a laboratory (Section 9.2). Finally, most experiments on exo-atmospheric systems can be done on the ground, e.g., using evacuated pipes for propagating the beam, and without requiring safety precautions which are dramatically more stringent than those required by the operation of typical accelerators used for scientific research.

• Endo-atmospheric beam technology is very similar to the relatively highintensity (kA), relatively low-energy (MeV), beam technology used in military laboratories for the flash x-ray radiography of the detonation of conventional explosives and nuclear weapon's primaries [86, p.81-84], the generation of high-power radio-frequency or free-electron-laser beams, and the simulation of nuclear weapons effects [30]. On the other hand, this technology has only few civilian applications, such as industrial radiography, electron-beam welding, and possibly future inertial confinement fusion drivers and very high-energy particle accelerators [133]. Therefore, the development and demonstration of this technology is mostly done in military and national laboratories, as will be seen in sections 10.1 to 10.4. Nevertheless, there is significant overlap between these developments and those of conventional research accelerators, as is shown by the fact that both type of technologies are generally discussed at the same national and international scientific conferences, and published in the same technical journals. Finally, an additional reason for locating these experiments in military laboratories is that even relatively modest endo-atmospheric systems create special hazards because the total energy in typical beam pulses can easily be equivalent to the energy content of gram- to kilogram-amounts of high-explosives.

The purpose of this report is to review the physics of high-intensity highenergy particle beam propagation. The discussion of exo-atmospheric systems could therefore be very brief since (as noticed in section 3.1) there is in principle no scientific obstacle to propagating a neutral beam over long distances in the near-vacuum of outer-space. We will nevertheless address some of the critical issues related to these systems, even though they are more of a technological than physical nature. This is because the development of exo-atmospheric beam weapons is in many ways linked to those of endo-atmospheric ones, and because their development illustrates the very strong interdependence which characterizes civilian and military particle accelerator research, as well as the importance of informal international collaborations and scientific exchanges (including between "enemies") in relation to the development of advanced weapons systems.

Chapter 9

Neutral particle beam propagation experiments

9.1 Neutral particle beam technology development

According to section 3.1, what is required to focus a stream of neutral particles on a 1 m target at a distance of 1000 km is a beam with an initial radius of 20 cm and an emittance of 2×10^{-7} m·rad.¹ As a charged particle is needed in order to be accelerated by electromagnetic means, the general technique is to start from a negative-ion source producing a low-energy, low-emittance beam of H⁻ or D⁻ atoms, which is then injected into an accelerator whose main quality is to increase the energy of the ions to about 100 MeV without unduly increasing the emittance of the beam. At the exit of the accelerator this high-brightness beam is very precisely focused on a target by a magnetic beam-steering optics, and then passed through a neutralizing cell in order to remove the extra electron (without increasing the beam emittance) so that the final beam is neutral.

Most of the basic technologies necessary for building such a system have been invented, built, and tested between the late 1970s and the early 1990s. This is what will be summarized in the next subsections:

¹Chapter VII and VIII of the Los Alamos Accelerator Technology Division 1978 progress report is describing a number of features associated with a system based on a 20–100 mA, 50–500 MeV beam with such an emittance [96, p.24-77].

9.1.1 The ion source

The first advance advance which made the concept of a neutral particle beam weapon scientifically feasible was the invention of a sufficient low-emittance negative ion source by the group of V.G. Dudnikov in the USSR [88, 89]. This pulsed surface-plasma ion source was quickly adopted world-wide, and Los Alamos soon demonstrated its superior performances relative to previously existing sources [90, p.117], [91].

9.1.2 The injector

The second major advance was again a Soviet invention. It solved the problem of injecting into a linear accelerator a low-energy low-emittance beam while maintaining its brightness. Moreover, this new injector was very compact and rugged. It is so-called "radiofrequency quadrupole" (RFQ), which, in combination with the Dudnikov high-brightness H⁻ source, led to speculations in the years 1978-1980 that the USSR might have had a considerable advance in particle beam weapons technology. However, while development of RFQ technology started in Russia in 1970 already, it only reached maturity around 1977, about the time when Los Alamos started its own RFQ programme [92].

In fact, it is in 1978 that a new *Accelerator Technology* (AT) division, headed by Edward A. Knapp, was formed at Los Alamos. The first step in the development of a neutral particle beam system for possible deployment in space, code-named "White Horse," was to build a 100 mA, 5 MeV accelerator test stand, which could be scaled up to about 50 MeV for outer-space re-entry-vehicle/decoy discrimination, and later to about 500 MeV for boost-phase or mid-course intercept of ballistic missiles. This accelerator test stand (ATS) was to integrate in a test-bed a Dudnikov H⁻ source, a RFQ to reach an energy of about 2 MeV, a drift-tube linear accelerator section to increase the beam energy to 5 MeV, and beam diagnostic equipments. This relatively small and low-cost system was to be supplemented by several collaborative undertaking on related military or civilian projects. This is why Los Alamos was glad to accept a proposal form CERN, reported in the 1980 AT division progress report [90, p.36]:

"(CERN) in Geneva, Switzerland, has asked the AT division to cooperate in the design and construction of an RFQ linac. This linac would replace the [...] injector [...] used with the "old" linac for the CERN proton synchrotron. [...] The plan is to carry out the mechanical design and assemblies at CERN, and then send them to Los Alamos

for machining of the pole tips."

The reason why CERN needed Los Alamos for building an RFQ is that the precise machining of its pole tips required a computer-controlled milling-machine of a type that was only available in a nuclear-weapons laboratory such as Los Alamos. Reciprocally, Los Alamos needed CERN as it provided a test-bed for coupling an advanced RFQ injector to a high-energy linac, which, moreover, happened to be the most recent and advanced in the world at the time.

Therefore, while the first successful high-power operation of a prototype RFQ with beam was obtained in February 1980, the first operational RFQ built at Los Alamos was shipped to CERN and installed on its new linac, while the second to become operational was installed on the Los Alamos accelerator test stand in November 1982 [93, p.53].

9.1.3 The accelerator

A major achievement of the Los Alamos accelerator technology division has been to reach, in 1979, a quantitative understanding of emittance growth in linear accelerators [94], showing that there is a lower limit to the emittance of such accelerators [95]. This understanding had been made possible by numerous exchanges between Los Alamos and many other institutions, including the CERN laboratory in Geneva. As an example, we cite a few sentences of the section on emittance growth of the 1978 Los Alamos accelerator technology division progress report [96, p.63,64,71]:²

"The new 50-MeV injector linac of CERN is the latest of this type proton linear accelerator to be commissioned in the world. [...] Preliminary results from CERN during the early summer 1978, using the first tank at 10 MeV, indicated larger than anticipated emittance growth. Knowing our urgent need for verification of the design approach for the FMIT project, the CERN Linac Group graciously invited our participation in the commissioning of the full machine. An on-site collaboration afforded us the opportunity to reach a level of understanding impossible to achieve at conferences or by letter. [...] We very much appreciate the complete openness, candor, and hospitality of the whole CERN linac group. Their willingness to let us use

²We stress that these quotes are from a 47-page long chapter entirely dedicated to the discussion of the design of an accelerator and of a beam-steering system for possible use as a particle beam weapon in the context of the "White Horse" project.

their raw data, before they had time to publish their results, was the key that enabled us to answer our basic questions in the urgent time scale imposed by current projects."

9.1.4 The beam focusing and steering optics

A major issue in a space-based neutral beam system is the ability to focus the beam into an acceptably small spot at some distance, and to provide a steering capability for aiming the beam. Using the ray-tracing computer programme TURTLE (a typical particle beam optics development tool devised by a collaboration of accelerator physicists from FNAL, SLAC, and CERN), the Los Alamos accelerator group was able to show in 1978 that a 50-meter long system of bending magnets and solenoids was able to focus 91% of a few 100 MeV hydrogen beam within the desired radius, starting with an initial radius of 0.2 m and an emittance of 2×10^{-7} m·rad [96, p.52–62]. An optical system with these characteristics was ultimately built and successfully tested in 1990 at the Argonne National Laboratory near Chicago.

9.1.5 The neutralizing cell

The final part of a neutral particle beam accelerator system, the neutralizing cell in which the extra electron is detached from the accelerated ion to form a beam of neutral atoms, is possibly the most controversial component of the whole system. This is because simple techniques (such as passing the beam through a foil or a gas to strip-off the extra electron) are likely to significantly increase the emittance of the beam and therefore to unduly decrease its brightness, at least for the most demanding applications of outer-space weapon systems. The most promising technique is therefore that of laser photodetachment, which is potentially 100% efficient rather than limited to about 55% as with collisional processes. High efficiency in outer-space is very important since any degree of incomplete neutralization of the beam could result in charging the orbiting accelerator, ultimately causing arcs that could lead to self-destruction. Moreover, it could be that by means of a multiphoton detachment process the excess electron could be removed without increasing beam emittance [97]. However, the kind of laser required for this purpose would add a considerable level of complexity to a space-based particle beam device, so that the whole subject of neutralization is still an open issue, despite constant progress [98, 99].

9.1.6 Summary

The developments presented in this section clearly show that the kind of accelerator and beam optics required for a neutral particle beam weapon can be built. Therefore, they established the scientific and technical feasibility of such systems. However, they does not prove their practical engineering feasibility, namely they do not demonstrate that a complete system (including power supplies, cooling, and many ancillary equipments) can be put in orbit and operated in outer-space. This is where the specific developments described in the next two sections come in.

9.2 BEAR and GTA at Los Alamos National Laboratory

Until 1983 the development of neutral particle beam weapon's technology and systems was made in the form of small, relatively low-cost, and mostly "paper" research programs. This was because (as shown in the previous section) the much more costly civilian research programs related to fundamental research could be used to develop and build all the key components of such systems, and that even international laboratories such as CERN, located in a neutral non-nuclear-weapon state, could be used for testing key component in full-scale accelerators.³

For this reason, the accelerator test stand (ATS), extensively referred to in the previous section, was sufficient to provide first hand experience on the most crucial components of a neutral particle beam system, and was even able to demonstrate reliable operation at 170 mA and 5 MeV, making it the brightest high-current H⁻ beam in the world [102, p.3].

Nevertheless, with the advent of President Reagan's Strategic Defense Initiative, neutral particle beam weapons were to be evaluate in competition with other directed-energy systems such as high-energy lasers and nuclear-pumped x-ray lasers. This lead to the definition of a comprehensive, national neutral particle beam research and development program lead by the Los Alamos laboratory, described in a September-1986 brochure [102], and related technical reports [103]. The objectives of this program were: (i) to provide the necessary basis for a decision by 1992 to build a space-based neutral particle beam system to be used as

³The same will happened in the mid-1980s, and still continue today, with the development of antimatter technology where U.S. scientists from weapons-laboratories or working on defence-contracts have essentially free, unlimited access to all of CERN's antimatter facilities [84, 100, 101].

a decoy/warhead discriminator (near term goal); (ii) to develop the technology in stages to ultimately build a neutral particle beam weapon capable to provide a rapid hard kill of enemy warheads (far term goal). To meet these objectives and more directly the first one the essential elements of the program were:

- 1. The *Integrated Space Experiment 1* (ISE-1) and the *Beam Experiment Aboard Rocket* (BEAR);
- 2. The *Ground Test Accelerator* (GTA) and the *Technology Program*.

The near-term goal was therefore to use the space shuttle to launch, in 1991, a 50-MeV-accelerator-based system into space (ISE-1), a quite ambitious objective. This was to be preceded by the suborbital launch, in 1987, of a 1-MeV accelerator by a single-stage Aries rocket. In this context, the GTA was to be representative of what was actually to be placed into orbit in ISE-1, while the BEAR payload was basically to be a ruggedized and less powerful version of the ATS, packed into a cylindrical volume of 1 m diameter and 7 meter length, together with diagnostic instrumentation.

However, as a consequence of the January 28, 1986, *Challenger* space shuttle disaster and funding constraints, the Integrated Space Experiment (ISE-1) was cancelled, and Los Alamos was asked in December 1987 to complete BEAR on an accelerated schedule with limited funding [104, p.25]. The BEAR payload was launched 200 km into space on July 13, 1989, and several accounts, e.g., reference [104], as well as the final report, i.e., reference [105], described the experiment as a success:

"The US Department of Defense's Strategic Defense Initiative Organization is sponsoring the development of neutral particle beam (NPB) technology for strategic defense applications. The first step in demonstrating the functioning of an NPB in space was the development and launch of the Beam Experiments Aboard a Rocket (BEAR) in New Mexico in July 1989. A government, laboratory, and industrial team, under the technical coordination of Los Alamos National Laboratory, designed, developed, and tested the BEAR payload. The primary objective of BEAR was the operation of an NPB accelerator in space. The payload was also designed to study (1) the effects on the space vehicle of emitting an NPB and associated charged beams into the space environment; (2) the propagation and attenuation characteristics of

an NPB in space; (3) the dynamics of the charged particle components of the beam in the geomagnetic field; (4) the effects of neutral effluents from the vehicle; and (5) any anomalous or unanticipated phenomena associated with operating an NPB in the space environment. The BEAR experiment successfully demonstrated operation of an NPB accelerator and propagation of the neutral beam as predicted in space, obtained first-of-a-kind NPB physics data, and demonstrated the ability of the BEAR accelerator to survive recovery and to continue operating normally. No unanticipated phenomena were encountered that would significantly delay further development of NPB technology for defensive, space-based weapon systems." [105]

On the ground, despite the cancellation of the first (and thus subsequent) integrated space experiment(s), construction of the GTA proceeded more or less on schedule, and the accelerator was commissioned in 1992, producing a 24 MeV, 50 mA beam with a 2% duty factor [106]. Consistent with the design report, [103], and other reports, e.g., [102, 107], work on GTA and related equipments, such as the magnetic optics, proceeded in collaboration with numerous laboratories and universities (e.g., the Oak Ridge, Lawrence Berkeley, and Argonne national laboratories, the Northeastern University and the University of Texas) as well as with the industrial contractors associated to the project. In particular, a state-of-the-art RFQ was built at Los Alamos and delivered to serve as a proton source in the Superconducting Super Collider (SSC) expected to be built in Texas [107, 108]. Similarly, development and testing of the magnetic optics components were done at the Argonne and Lawrence Berkeley laboratories.

However, although all its components had been built, and many of them successfully tested, the GTA was never fully assembled, and its construction abandoned at the end of 1993 [108]. The floor space was later used for assembling and testing the Low Energy Demonstration Accelerator (LEDA) of the Accelerator Production of Tritium (APT) project [109]; various equipments and spare parts were reused in other projects; and finally the GTA accelerator itself was donated in 2004 to the University of Indiana for its Low Energy Neutron Source (LENS) facility, to be used as a training ground for scientists who will later work at the \$1.5 billion neutron source to be completed in 2006 at Oak Ridge [110]...

9.3 Emerging neutral beam technologies

As recalled in the previous section, the years immediately following the collapse of the Soviet Union coincided with the abandonment of the most visible components of the U.S. national neutral particle beam research and development program: the ISE experiment and the GTA accelerator. Nevertheless, this did not mean that interest in neutral particle beam was lost, neither that development stopped there. In particular, the numerous told and untold reasons for terminating an attempt to demonstrate the viability of a neutral particle beam system in outer-space were much more of a technical and political nature than of a fundamental one. With a successful proof of principle experiment such as BEAR, there was no really compelling scientific reason to make another space-based experiment which would not have added very much to the understanding of the underlying physical issues. In fact, problems such as developing an appropriate kW to MW class energy source for the whole system, a suitable cooling system for the accelerator, or a highly efficient beam neutralizer, would not have much benefited from a crash-program to put GTA into outer-space.

The points to be stressed are therefore:

- 1. That the accelerators and associated technologies for neutral beam weapon systems are so closely related to those of accelerators and detectors used for fundamental nuclear and elementary particle research that their development does not need to be done in military laboratories;
- 2. That the specific characteristics of neutral particle beams for military applications such as ballistic missile defense should be discussed in relation to the full range of technologies available for accomplishing similar decoy/weapon discrimination and/or target destruction objectives [78].

Indeed, the most important and almost unique advantages of high-energy particles are their ability to penetrate deeply into any target and to interact strongly (that is by inducing nuclear reactions) with any substance. This implies that the potential damage can be considerable, and that even for very low-intensity beams the secondary particles emitted in the nuclear interactions with the materials in the targets provide a signal giving a lot of information on their composition. This is illustrated by the current method which uses background cosmic-ray particles as a natural beam for the remote analysis of the elemental composition of artificial satellites [111]. While this method requires times on the order of months or years to integrate sufficient events to achieve useful data, directing a modest beam of accelerated particles at a given spacecraft would achieve the same result in a fraction of a second.⁴

⁴This requires, of course, the use of very sensitive and clever techniques for detecting the secondary particles emitted by the target, and for discriminating them against the cosmic-ray background, something that can only be compared to the skill required to design the detectors

Considering that it is most probably easier and less expensive to destroy a ballistic missile or a spacecraft by means of some kind of a kinetic interceptor than by either a high-energy laser or particle beam, the most potent application of a space-based particle beam is quite certainly that of warhead/decoy discrimination. This is possibly why this application had been assigned in priority to space-based particle beam systems starting 1986 in the United States (see, e.g., references [102] and [103], where it was stated that a discriminator/weapon decision was to be made by 1992). The remaining question to answer before designing and possibly deploying such discriminators is therefore whether there could be any strong competitor on the design horizon, of which two can easily be identified:

- 1. Antimatter beams. While a neutral hydrogen beam containing 5 to 10 MeV protons would be sufficiently energetic to strongly react with the surface of a target, a beam with an energy of at least 50 to 100 MeV is necessary to penetrate inside, or to generate sufficiently many neutrons on the surface, in order to determine whether there could be a nuclear warhead within. If instead the beam would consists of low-energy antihydrogen atoms, the antiprotons would spontaneously annihilate on the surface, generating several high-energy pions for every antiproton hits, which would deeply penetrate into the target and strongly interact with the materials. An antihydrogen beam would therefore enormously simplify the design of the accelerator, which could operate at a much lower beam energy and current than for conventional hydrogen beam. Therefore, the technological burden would be transferred to the antimatter technology, which, however, is under intensive development since more that ten years [80].
- 2. Superlaser beams. Comparisons of the relative ability of neutral particle beam and laser systems for discriminating between reentry vehicle and decoys show that particle beams can typically discriminate about hundred times as many objects as can lasers, and do so with significantly greater certainty [112]. This applies, however, to lasers with relatively low peak power. The recent invention of "chirped pulse amplification," which provided a factor of one million (i.e., 10⁶) increase in the instantaneous power of lasers, enabled tabletop lasers to produce nuclear reactions directly [113]. Therefore, superlaser beams combine the ease in steering and focusing of optical laser beams with the capacity of particle beams to generate high-energy secondary particles in distant targets, which gives them the ability to "x-ray" remote objects and discriminate whether they are warheads or decoys [78].

and analyse the results of sophisticated high-sensitivity nuclear or elementary-particle physics experiments.

One can therefore conclude that neutral particle beams provide a credible option for discrimination, but that this option should be constantly compared to emerging alternatives which arise as technology advances. In particular, it may happen that the laser system required to neutralize a negative hydrogen beam could in fact be of a complexity comparable to that of a superlaser able to do the same discrimination task on its own... But it would then be necessary to assess that further advances in antimatter technology would not require a complete reevaluation of the possible military uses of antimatter, both in offensive and in defensive weapons (see, [84, 100, 101, 80] and references therein).

Conversely, if some major scientific or technical advance is made in accelerator technology, such as very-high-efficiency superconductive acceleration and radio-frequency generation, very-high-brightness laser-acceleration of neutral-particles, etc., neutral particle beams may find again their leading position as a potential rapid hard-kill system, simply because of the intrinsic strongly-interacting nature of high-energy particles.⁵

 $^{^5}$ The abstract of a typical comparative study (possibly biased in favor of particle beams) summarized this fact as follows: "This report explores the role of directed energy weapons (DEWs) in theater defenses. For ranges shorter than 200-300 km they are much cheaper than space-based interceptors (SBIs); they are competitive with ground-based interceptors (GBIs). For inter-theater ranges of ≈ 1000 km, lasers are competitive with the SBIs, but NPBs are significantly cheaper than either. For nominal laser and space-based interceptor (SBI) costs, lasers are strongly preferred for ranges under 300-500 km. For ranges 700 km, SBIs have a slight advantage. Neutral particle beams (NPBs) appear dominant for ranges over 400-1000 km" [114].

Chapter 10

Charged particle beam propagation experiments

10.1 ATA at Lawrence Livermore National Laboratory

The purpose of the construction and operation of the Advanced Test Accelerator facility (the ATA) at the LLNL, as well as its basic characteristics, have been described in a number of informal, e.g., [115, 24, 116, 117], and more technical, e.g., [118, 119, 120], papers and reports. Summarizing from these publications:

The main uncertainty in the concept of charge-particle beam weapons is whether it is feasible to propagate an intense self-focused electron beam through the atmosphere. That is, an electron beam held in tight focus by its own magnetic field. To conduct a comprehensive program of electron-beam propagation experiments, LLNL has constructed between 1978 and 1982 a 50 MeV, 10 kA, linear accelerator (the ATA) at its high-explosive test location, *Site 300*, which is well equipped for managing experiments with unusual hazards.

Together with its associated program of beam propagation physics, the ATA represents the largest single component of the Defense Advanced Research Agency (DARPA) particle-beam technology program, whose aim is to establish the feasibility of particle beam weapons. The prime goal of the Department of Defense particle-beam technology program is to resolve what is and is not possible in beam propagation. Accordingly, the goal of the ATA is to develop an

experimental capability that can resolve critical questions about beam propagation physics in a timely and cost-effective fashion.

A first generation of particle-beam weapons will emphasize short-range applications. Potentially first applications of particle-beam weapons may be for the defense of large ships against cruise missiles. Another early use may be for terminal ballistic missile defense of hardened sites such as missile silos or national command authority centers. The short range, which reduces the sensor burden on search and fire-control radars, demands the high lethality that particle-beams possess. Boring its way out to targets at a rate of a kilometer per millisecond, the beam can deposit megajoule of energy almost instantaneously. Consistent with fire-control system considerations, beam weapons can have the capability of engaging tens of targets per second. With such characteristics, charged-particle beams are particularly well suited to counter small, very fast, highly maneuverable threats.

Photographs of the completed 200-meter-long ATA facility, as well as drawings of the 80-meter-long underground experimental tank are shown in reference [116]. Also visible is the 4-meter-thick shielded door which can be moved aside for beam experiments in open air. For such open air experiments the beam is directed towards a staging area where it may interact with various targets after propagating in free air over distances which are only limited by the topography of the ATA site, located in a shallow valley at *Site 300*.

The main characteristics of the ATA in relation to his primary purpose, the study of endo-atmospheric beam propagation and interaction with military targets, are as follows:

• Beam energy: 50 MeV

An energy of 50 MeV means that that the electron beam is fully relativistic but of an energy still substantially below the 1'000 to 10'000 MeV that are needed to have a beam power on the order of the Nordsieck power, which is the required for propagating a distance of about one radiation length in open-air in a single pulse (Figure 4.3). This means that the experiments at ATA will be done under rather difficult conditions, which has the advantage that the results will easily extrapolate to higher energies. In this respect, it is important to recall that the main difficulties with particle acceleration is in the low energy section: as soon as an electron beam has reached an energy of 10 to 100 MeV it is easy to inject it into a betatron and further accelerate

it to higher energies. An example of such a betatron, designed to accelerate the 10 kA ATA beam from 50 to 250 MeV, is given in reference [121].

• Beam current: 10 kA

A current of 10 kA is on the order of the critical current given by equation (5.8), which corresponds to the maximum current for self-pinched propagation through the atmosphere a sea-level pressure.

• Pulse length: 70 ns

A pulse length of 70 ns is adequate for studying nose erosion and tail losses during propagation, as well as the convective nature of major instabilities such the hose instability.

• Burst rate: 1 kHz — Average rate: 5 Hz

A maximum repetition rate of 1'000 Herz, and an average rate of 5 Herz, imply that every second five successive pulses separated by a time-delay between 1 and 200 milliseconds can be sent into the experimental tank or into the atmosphere. This enables to study hole boring and stability of subsequent pulses through the low-density plasma generate by preceding pulses in reduced-density or ground-level air.

• Lethality: 35 kJ/pulse

The is only 3.5 percent of the 1 MJ energy which would be delivered by a 100 ns, 10 kA, 1 GeV beam pulse, i.e., the energy equivalent of about 0.25 kg of TNT, which is considered to be on the order necessary to destroy a typical target. Nevertheless, this is sufficient to test the lethality of the beam on numerous targets without completely destroying them and the sensors used in the measurements.

The accelerating principle used in the ATA is *magnetic induction*, a technology traditionally used in circular accelerators such as the betatron, which was pioneered and developed for use in linear accelerators at the Lawrence Livermore National Laboratory by N.C. Christofilos [122].

The construction of the ATA started in 1980. The first tests of the electron gun (injector) began in November of 1982, and its full 10 kA, 2.5 MeV, beam was delivered to the ATA main accelerator in January 1983.

The ATA started operating at its full design specifications of 10 kA and 50 MeV in July 1984. However, the beam current was was found to be strictly limited by instabilities within the accelerator so that only very uniform beam pulses could

be accelerated to full energy when injected into the 85-m-long main accelerator structure.

The most serious such instability, termed *beam break-up* (BBU), is a very rapid growth of any beam's transverse displacement to a disruptive amplitude. A radical cure to this problem was found and tested in the early 1985 using another lower-energy induction accelerator, the Experimental Test Accelerator (ETA), [123, 124]. The idea was to fill the accelerator with benzene gas at a pressure of 10^{-2} Pa, corresponding to an altitude of 80 to 120 kilometer above the Earth, and to created a plasma channel by sending a low-energy laser pulse through it. This proved to be very successful, the channel providing an electrostatic guide for the beam all the way through the accelerator [125]. Moreover, this breakthrough provided a way to greatly simplify the construction, and to reduce the weight, of future linear induction accelerator. Indeed, quoting from an October 1985 review of the ATA progress:

"Clearly, the laser guiding technology gives a tremendous improvement in accelerator performances as well as simplifies accelerator operation and future construction (i.e., no longer needed are transport solenoid or steering magnets)" [126, p.3145].

The final confirmation of the full and reliable operation of ATA by the use of the laser guiding transport technique was given on September 1986, [127, 128]. From then on the ATA could be used for what it had been built for: to investigate the feasibility of an intense charge-particle beam as an endo-atmospheric point-defense weapon. It turned out that the answer to one basic question of principle, namely that the propagation of the beam over long distances in open air is possible, came very soon.

Indeed, in his State of the Laboratory statement of 1987, the director of LLNL was able to highlight:

"A major accomplishment in the laboratory's beam research program was the first demonstration of open-air propagation of an electron-beam. Using the Advanced Test Accelerator (ATA), researchers were able to tailor the electron beam to permit stable propagation in the open air" [129, p.3].

In the Beam Research section of the same annual report, the following details were given:

"Recently we successfully transported a high-intensity, 50-MeV electron beam from our Advanced Test Accelerator (ATA) into conditioning and diagnostic cells and then into free air. This test of stable beam propagation in free air is the first of its kind at this energy, level of beam current (5 to 10 kA), and pulse rate (1 Hz). We have studied carefully the effects of beam parameters upon stability in air and have begun measurements of ancillary phenomena that will be important in assessing the practicality of using high-intensity electron beams as tactical weapons" [130, p.54].

However, none of the experimental details concerning these propagation experiments appear to have been published. Neither will there be any more detailed publications on the ATA and its uses over the following years until today. In particular, there is no information whether the ATA beam has been used as an input into another, most probably circular, accelerator to increase its beam energy from 50 MeV to 500 MeV or more [121, 131, 132]. The only subsequent open publications related to the ATA are those concerned with its use as a driver for a free-electron laser, e.g., [133], or publications related to technological developments which may be used to upgrade the ATA or to build highly reliable and efficient components for a new generation of high-current high-energy accelerators, e.g., [134].

In conclusion, if we take the above statements for granted, we have to assume that the ATA project has succeeded in meeting its stated goals. This means, in particular, that single pulses must have propagated in a stable manner in free air over a distance of at least one Nordsieck length, equation (4.27), i.e., about 20 meters according to the calculations made at the end of Section 4.3. Since ATA is able to fire five closely spaced pulses in a single burst, operation in this burst-mode must have allowed to verify that the stable propagation of a tightly focused beam is possible up to a distance of about 100 m. According to the available drawings of the ATA facility, e.g., the cover page of the brochure [115], this range is about the distance between the exit port of the ATA and the focal point of the out-doors staging area.

10.2 RADLAC at Sandia National Laboratory

The main advantages of linear induction accelerators such as the ATA used for beam research, or such as the FXR, DARHT, or AIRIX used for flash x-ray radiography, are their intrinsic simplicity and capability to produce high quality

beam pulses under reliable conditions. However, while such accelerators are well suited for research applications, they are very heavy and bulky, and therefore not suitable for applications in which relatively compact and light-weight accelerators are required.

One alternative technology has been successfully developed by A.I. Pavlovskii in the Soviet Union, with possible applications to *linear induction accelerator without iron* [135, 73], and *pulsed air-cored betatrons* [136]. This technology, which does not use ferrite- or iron-loaded cavities, was subsequently developed in the United States, and the first device based on this principle was built and successfully operated at the Sandia National Laboratory [137]. The current and energy achieved in this accelerator, called RADLAC-I, were of 25 kA and 9 MeV with an average accelerating gradient of 3 MV/m. This accelerating gradient is substantially larger than that of the ATA (about 0.5 MV/m) which implies that the RADLAC is a promising candidate for a compact high-power accelerator. Moreover, the RADLAC can operate at high repetition rates since it is not affected by the classical beam breakup (BBU) instability, so that laser guiding of the beam in a laser-generated channel within the accelerator is not necessary [137, p.1185].¹

The RADLAC technology was substantially improved during the 1980s and the construction of RADLAC-II initiated. This accelerator consists of two successives accelerating modules called RIIM. Using such modules in succession a beam can be accelerated to higher and higher energies. In 1985 RIIM was capable of reliable operation at output levels of 40 kA and 9 MeV [139].

With the RIIM operating, RADLAC-II could be assembled and beam propagation experiments using its 40 kA, 18 MeV beam were soon successful [140]. In early 1986 the beam was extracted, without significant losses, and propagated into a magnetic-field-free, air-filled experimental tank. At a pressure of 1 atm the beam propagated straight without oscillations, and the radius was measured to be about 0.75 cm, somewhat smaller than the 0.9 cm beam radius within the accelerator. The RADLAC-II beam was then conditioned in a 16-m-long, ion-focused region, and was allowed to propagate outside the accelerator building in open air where it propagated in a stable manner for quite a distance. As a matter of fact, figure 9 of reference [140] is an open-shutter photograph of the RADLAC-II beam propagating outdoors at night. The Manzano mountains of New Mexico are visible in the background.

Subsequent publications gave no further details on out-doors propagation experiments. Nevertheless, research and development did not stop there, as is

¹For a general discussion of this technology, and its applications to both linear and circular accelerators in the United States and in Russia, see the review [138].

indicated by the summary presented at the subsequent DARPA conference [141]:

"RADLAC program activities are reviewed. The work is broadly categorized under lead pulse stability (LPS), channel tracking, and Recirculating Linear Accelerator (RLA) activities. In LPS activities, stable, open-air propagation of the RADLAC-II beam was demonstrated over ranges longer than a Nordsieck length. These shots were coordinated with the activities of other experimenters measuring beam induced emissions, and demonstrated that RADLAC-II could be fired on a predetermined schedule to allow numerous, coordinated, and geographically widespread measurements to be made. Since those experiments, improvements in the RADLAC-II accelerator, ion-focus regime (IFR) beam conditioning cells, and matching of the accelerator beam to those cells have produced a beam which should allow greater than 20 betatron wavelengths in a Nordsieck length and saturation of hose growth to be observed. Channel tracking activities have included continued hardware development on the RADLAC-II Module (RIIM) for pulse-to-pulse channel tracking, the design of a laser for conductivity channel tracking, and demonstration of a crude beam director for a high current beam. Codes which allow channel tracking simulations to be done have also been developed. Pulsed power and beam transport experiments on the Recirculating Linac have led to hardware and techniques which will allow demonstration of beam recirculation of a high current beam this year and a recirculating linear accelerator next year. These transport schemes and pulsed power developments can be extended to higher energies and a conceptual RLA for Navy charged particle beam weapon (CPBW) applications has been developed."

As well as at the 1987 SDIO/DARPA Services Annual Propagation Review [142]:

"The RADLAC program encompasses high power electron beam propagation experiments and accelerator development, both for advanced propagation experiments and to develop compact accelerator options for future charged particle beam weapons (CPBW). Propagation experiments include conditioning cell and lead pulse stability (LPS) experiments on RADLAC-II, and channel-tracking experiments on IBEX. The RIIM accelerator was used for two-pulse accelerator experiments to explore two-pulse configurations for RADLAC-II. The

ion-focused regime (IFR) transported, recirculating linear accelerator (RLA) experiment is aimed at future CPBW compact accelerator development. This paper briefly outlines recent work in these areas."

Concerning the stable open-air propagation of the RADLAC-II beam, it is remarquable that it is was demonstrated in 1986 already, [140], that is possibly one year earlier than the same experiment with the ATA beam, [129, p.3] and [130, p.54]. This illustrates both the maturity of the RADLAC technology, and the level of the inter-US competition between national laboratories.

As for the significance of the RADLAC-II open-air experiments in comparison to the corresponding ATA experiments, it should be remembered that what matters most in first order is beam power, as is shown by the elementary solution (4.26) to the Nordsieck equation (4.24). For ATA the initial beam power is $P_0 \approx 0.5$ TW, and for RADLAC-II $P_0 \approx 0.72$ TW. Therefore, according to Nordsieck length's approximation, (4.27), RADLAC-II should have a single-pulse range on the order of about 30 m, instead of about 20 m for ATA. However, if the calculations are made by computer-integrating the complete beam envelope equation (4.18) using Molière's theory of multiple scattering [32] and detailed energy-loss models, it turns out that both RADLAC-II and ATA have about the same e-fold range of approximately 22 m. In other words, while Nordsieck's equation provides a good first approximation (especially for beams of high-energy particles), computer simulations are indispensable in the relatively low-energy domain in which both ATA and RADLAC-II are operating.

A final important conclusion deriving from the RADLAC-II stable propagation experiments is that the plasma generation current (5.8), which should theoretically limit stable propagation to currents less then about 10 kA, does not appear to be so critical, since the RADLAC-II beam intensity is of 40 kA.

10.3 LIA-10 and LIA-30 at Arzamas-16

As it originally started in the Soviet Union, e.g., [135, 136, 73], it is obvious that the development, and most certainly the use for beam propagation experiments, of iron-free linear induction accelerators continued in Russia. Indeed, the LIA-10 accelerator of the 1970-1980s was upgraded to yield 50 kA for a 25 MeV pulse of 20 ns duration in 1993, and the construction of a new accelerator, LIA-30, producing a beam of 100 kA at 40 MeV, initiated [143].

However, there are no published results on long-range beam propagation experiments using these facilities. Moreover, while there is substantial published

work on Russian beam propagation experiments through low-pressure air or even laser formed channels, e.g., [144, 145], there appears to be no open publications available on experiments similar to those made with ATA and RADLAC.²

10.4 PHERMEX at Los Alamos National Laboratory

A third technology suitable for making compact high-power accelerators is the more conventional standing-wave radio-frequency linac technology used in most high-energy linear accelerators built for fundamental nuclear and elementary-particles research. Using this technology, it is theoretically possible to accelerate a 10 kA beam pulse from 10 to 1000 MeV in a 30-meter-long linear accelerator [146].

This technology was in fact used in the first high-power flash x-ray facility, the PHERMEX accelerator complete in 1963, built at the Los Alamos National Laboratory to study the implosion of nuclear weapon's primaries [147]. As this facility was expected to be superseeded by more powerful induction linacs (such as the DARHT, which is now operating) it was suggested in the early 1980s that PHERMEX could possibly be upgraded and used to study the endo-atmospheric propagation of electron beams [23].

While the RF-linac technology has a few disadvantages compared to the induction-linac technology (e.g., a relatively short pulse length), it has an intrinsic high repetition rate and multi-pulse capability. Besides, PHERMEX is located "in a blast-proof building at a remote, controlled access site [where] a clear line of site of approximately 2000 meters exists" [23, p.2].

In fact, some preliminary propagation experiments were performed using the available beam [148], and PHERMEX was subsequently upgraded to operate in the 20 to 60 MeV energy, up to 3 kA intensity range which was anticipated to be theoretically possible [23, 149].

Emittance measurements for typical 300 to 500 A, 26 MeV, 3.3 ns micropulses were published [150], as well as several papers indicating that there are plans to inject the PHERMEX beam into a circular accelerator [151, 152, 132]. Besides increasing the beam energy, such an accelerator would have the advantage of

²The Rand Corporation report [145] mentions that: "A follow-on report will discuss Soviet research on the propagation of intense relativistic electron beams through higher-pressure air and gases ($P > 10^{-2}$ Torr)."

providing a means to accumulate and condition the beam pulses before sending them into the atmosphere with a suitably larger energy, current, and duration.

There are, however, no subsequent publications on these developments. In particular, it is not known whether or not PHERMEX is now used as an injector to a higher-energy circular (or even possibly linear, see [146, p.2]) accelerator, and there is no published information on related beam propagation experiments.

10.5 Proton and muon beams

So far we have only considered experiments in which high-intensity *electron* beams are generated, accelerated, and injected into the atmosphere. The main reason for this was that electron-beam machines with currents in the kiloampere range still appear to be the only available ones to study endo-atmospheric beam propagation over distances on the order of one or more Nordsieck lengths. Nevertheless, in view of the potentially larger range of *proton* versus electron beams, see Figures 4.2 and 4.3, and other interests such as ion-driven thermonuclear fusion, research on high-current proton beam sources suitable for injecting a multi-kiloampere pulse into an accelerator is under way since quite some times. This is illustrated, for example, by the 6.0-kA, 1.1-MV proton beam obtained at Cornell University Laboratory of Plasma Studies [153].

Similarly, considerable research is underway for producing high-intensity low-emittance *muon* beams for fundamental research [154]. If the techniques used for producing these beams could be extrapolated to yield sufficiently powerful pulses of muons, a single such pulse could in principle propagate (according to Figure 4.2 and 4.3) to ranges of up to several km in open air. The main problem with muons, however, is that they are short-lived particles, with a life-time τ_{μ} of only 2.2 microseconds at rest. Nevertheless, if the muons are accelerated, say to 1000 MeV (which since the mass of the muon is $m_{\mu}=105~{\rm MeV/c^2}$ corresponds to a Lorentz factor of $\gamma\approx 10$) they would be able to propagate to a distance of $\gamma c \tau_{\mu}\approx 6.6~{\rm km}$ before decaying. Therefore, in theory, a series of high-energy muon beam pulses could be used either to strike a target at a distance of tens of kilometers, or else to bore a channel in the atmosphere to guide a more powerful electron or proton beam to a distant target [80].

While such a concept may look very futuristic at present, it should nevertheless be seriously assessed in view of several synergistic factors which relate muon beam technology to other advanced beam technologies of importance to the subject of this report. For example, there is strong similarity between the techniques used to produce muons (see, e.g., chapters 2 to 4 in reference [154]) and those used to produce antiprotons (see, e.g., [84]): In both cases the simplest method consists of striking a production-target with a sufficiently high-energy proton beam to generate copious amounts of either muons or antiprotons during the collisions, to collect as many as possible of these particles with a magnetic lens, and to decrease their kinetic energy dispersion (i.e, to "cool" them) in order to form a sufficiently low-emittance beam, which can then be stored or directly used for some purpose.³ Moreover, if instead of producing the muons with a high-energy proton beam, a high-intensity electron beam is used instead, one is led to a system involving a multi-megawatt muon production-target driven by a multi-kiloampere electron beam, which requires the kind of technologies and experience associated with accelerators such as the ATA [155].⁴

In practice, the kind of muon production and cooling systems envisaged or under construction at present, e.g., [154, 157], are not expected to be fully operational before 2006 to 2010. Also, their muon yield will be orders of magnitudes below what would be needed to envisage concentrating a bunch of them into a pulse suitable for propagation in self-pinched mode over a significant distance in open air. Nevertheless, this situation is quite similar to that of antiproton "factories," which have increased (and are still increasing) their output by many orders of magnitude over the years.

³Another link between muon and antimatter technology, which was already mentioned in Chapter 8, is that antimatter is the sole portable source of muons, in the sense that upon annihilation every antiproton yields on average between 2 and 3 muons, which could be fed to a collecting and cooling system without needing a high-energy beam to produce the muons in the first place [80].

⁴The first author of this paper headed the ATA project for a number of years, see [24, 116]. It should be remarked that in an electron-beam based system, the same high-power electron accelerator could be used as a driver for either a free-electron-laser or a muon-factory, which would both provide a means to guide the more powerful electron-beam towards a distant target. For more examples of such synergies, see, e.g., [156].

Chapter 11

Conclusion

In this report we have reviewed the theory and the proof-of-principle experiments which have been carried out to demonstrate that high-intensity high-energy particle beam propagation in full or reduced-density atmosphere was possible, and that the range and stability of the beam pulses were in agreement with theory.

We have, however, not analysed the practical consequencies of these conclusions, which determine with certainty the range of physical parameters compatible with realistic high-power directed-energy particle beam systems; neither have we investigated the R&D related to the possible construction and deployment of such systems. These are the subjects of a companion report, of which only a small part, concerned with the radiological effects of directed high-intensity high-energy electron beams, has so far been published [158].

Nevertheless, by going through the theory and the details of several important experiments, we have followed several complete "research cycles," that is several paths going from some initial ideas to their verification by means of a suitable experimental program. In the present case the outcomes of these research cycles can be qualified as "scientifically successful," meaning that the technical feasibility of some concepts have been established. While this is important, it does not mean that the associated technologies should necessarily be developed and applied, which is precisely the motivation for writing this report.²

¹Particle beam weapons: A review and assessment of current R&D, Report ISRI-82-05, to be published.

²"And let us not forget that a great breakthrough in military technology, like the invention of the H-bomb, can quickly come back to haunt us." Hans Bethe, Physics Today, October 1978, p.13.

Bibliography

- [1] J.D. Lawson, The Physics of Charged-Particle Beams, (Clarendon Press, Oxford, 1977) 462 pp.
- [2] R.B. Miller, An Introduction to the Physics of Intense Charged particle Beams (Plenum Press, New York and London, 1982) 351 pp
- [3] Principles of Charged Particle Acceleration (John Wiley & Sons, New York, 1986) 820 pp. This book is available on the internet at http://www.fieldp.com/cpa
- [4] Charged particle Beams (John Wiley & Sons, New York, 1990) 820 pp. This book is available since 2002 on the internet at http://www.fieldp.com/cpb
- [5] M. Reiser, Theory and Design of Charged Particle Beams (John Wiley & Sons, New York, 1996) 612 pp.
- [6] J.D. Lawson, P.M. Lapostolle, and R.L. Gluckstern, *Emittance, entropy and information*, particle Accelerators, **5** (1973) 61–65.
- [7] H. Alfvén, On the motion of cosmic rays in interstellar space, Phys. Rev. **55** 425.
- [8] R.A. McCorkle, *Quasi-equilibrium beam-plasma dynamics*, Appl. Phys. Lett. **41** (1982) 522–523.
- [9] C. Robert Emigh, Statistical Beam Transport for high Intensity Ion current, in Proc. of the 1972 proton linear accelerator conference, Los Alamos, report LA-5115 (Los Alamos National Laboratory, November 1972) 182–190.
- [10] D. Keefe, *Research on high beam-current accelerators*, Particle Accelerators **2** (1981) 187.
- [11] J.D. Lawson, *Perveance and the Bennett pinch relation in partially neutralized electron beams*, J. Electron. Control **5** (1958) 146–151.

- J.D. Lawson, *On the classification of electron streams*, J. Nucl. Energy, **C1** (1959) 31–35.
- [12] G. Wallis et al., Injection of high-current relativistic electron beams into plasma and gas, Sov. Phys. Usp. 17 (1975) 492–506.
 S.E. Rosinskii et al., Mechanism of acceleration of ions on the front of ionization of a gas by relativistic electron beam, ZhETF Pis. Red. 14 (1971) 53–57.
- [13] E.P. Lee and R.K. Cooper, *General Envelope Equation for cylindrically symmetric charged-particle beams*, Particle Accelerators **7** (1976) 83–95.
- [14] W.H. Bennett, Self-Focusing Streams, Phys. Rev. 98 (1955) 1584–1593.
- [15] G. Benford and D.L. Book, *Relativistic Beam Equilibria*, Adv. in Plasma Phys. **4** (1971) 125–174.
- [16] E.P. Lee, *Kinetic theory of a relativistic beam*, Phys. of Fluids **19** (1976) 60–69.
- [17] R.J. Briggs et al., *Radial expansion of self-focused, relativistic electron beams*, Phys. of Fluids **19** (1976) 1007–1011.
- [18] E.P. Lee, *The charge transport problem*, report UCID-17380 (Lawrence Livermore National Laboratory, 1977) 9 pp.
- [19] M.P. Gough et al., *Bunching of 8–10 keV auroral electrons near an artificial electron beam*, Nature **287** (4 September 1980) 15.
- [20] Y. Kiwamoto, Propagation and Expansion of an Electron Beam Ejected from the Space Shuttle into the Ionosphere, report IPPJ-286 (Nagoya University, 1977) 6 pp.
 W.M. Neupert et al., Science on the Space Shuttle, Nature 296 (18 March 1982) 193–197.
- [21] R.M. Salter, Application of electron beams in space for energy storage and optical beam generation, RAND report P-6097, (Rand Corporation, Santa Monica, April 1978) 19 pp.
- [22] J.W. Beal, R.J. Briggs, and L.D. Pearlstein, *Beam Research Progress Recent Results and Status*, report UCID-16169 (Lawrence Livermore National Laboratory, 1972) 17 pp.

- [23] D.C. Moir et al., Suitability of High-Current Standing-Wave Linac Technology for Ultra-Relativistic Electron Beam Propagation Experiments, report LA-8645-MS (Los Alamos National Laboratory, 1981) 28 pp.
- [24] W.A. Barletta, *The Advanced Test Accelerator Generating intense electron beams for military applications*, Military Electronics/Countermeasures (August 1981) 21–26.
- [25] R.E. Hester et al., *Deflection of a high current relativistic electron-beam by a weak magnetic field in the presence of plasma*, report UCID-16597, Lawrence Livermore National Laboratory, 1974.
- [26] G. Schmidt, *Plasma motion across magnetic fields*, Phys. of Fluids **3** (1960) 961.
- [27] S. Robertson, *Propagation of intense charge-neutral ion beams in magnetic fields*, Proc. High Power Beams 81, M.J. Doucet ed, Ecole Polytechnique, Palaiseau, France 1981.
- [28] J. Denavit, *Collisionless plasma into a vacuum*, Phys. Fluids **22** (1979) 1384–1392.
- [29] S.E. Graybill and S.V. Nablo, *Observations of magnetically self-focusing electron streams*, Appl. Phys. Lett. **8** (1966) 18.
- [30] H.H. Fleischmann, *High-current electron beams*, Physics Today (May 1975) 34–43.
- [31] B. Rossi, *Theory of Electromagnetic Interactions*, Chapter 2 of High Energy Particles (Prentice-Hall, New York, 1952, 1961).
- [32] H.A. Bethe, *Molière's theory of multiple scattering*, Phys. Rev. **89** (1953) 1256–1266.
- [33] M.I. Haftel et al., *Radial expansion of a self-pinched beam with distributed energy*, Phys. Fluids **22** (1979) 2216.
- [34] S.S. Kingsep, *Mechanism of gas ionization by an intense electron beam*, Sov. Phys. JETP. **36** (1973)1125.
- [35] E.P. Lee, *Model of beam head erosion*, report UCID-18768 (Lawrence Livermore National Laboratory, 1980) 19 pp.
- [36] D.A. McArthur and J.W. Poukey, *Plasma created in a neutral gas by a relativistic electron beam*, Phys. Fluids **16** (1973) 1996.

- [37] J.R. Cary, *Production of plasma from diatomic gases by relativistic electron beams*, Phys. Fluids **23** (1980) 1005.
- [38] F.W. Chambers and D.M. Cox, Standard test case runs for the impulse monopole fieldsolver and conductivity generation model, report UCID-19213, Lawrence Livermore National Laboratory, 1981.
- [39] S.S. Yu et al., *Beam propagating through a gaseous reactor-classical transport*, report UCRL-82029 (Lawrence Livermore National Laboratory, 1979) 12 pp.
- [40] R.J. Briggs et al., *Electromagnetically induced plasma back current near* the head of a relativistic electron beam entering gas, report UCID-16594, Lawrence Livermore National Laboratory, 1974.
- [41] W.M. Sharp, Steady-state treatment of relativistic electron beam erosion, Phys. Fluids **23** (1980) 2383.
- [42] L. Spitzer Jr., Physics of Fully Ionized Gases (Interscience Publ., New York, 1956).
- [43] R.J. Briggs, *Two-Stream Instabilities*, Adv. in Plasma Physics **4** (1971) 43–78.
- [44] G. Benford, *Theory of filamentation in relativistic electron beams*, Plasma Phys. **15** (1973) 483–499.
- [45] L.E. Thode, Plasma heating by scattering relativistic electron beams: Correlations among experiment, simulation, and theory, Phys. Fluids 19 (1976) 831.
 K.M. Watson and S.A. Bludman, Statistical mechanics of relativistic streams. I Phys. Fluids 3 (1960) 711.
- [46] H.E. Singhaus, Beam-Temperature Effects on the Electrostatic Instability for an electron beam penetrating a plasma, Phys. Fluids 7 (1964) 1535.
- [47] J.A. Nation and R.N. Sudan eds., Laboratory of plasma studies, Proc of the 2nd International Topical Conf. on High Power Electron and Ion Beam (Cornell University, Ithaca NY, 3-5 oct 1977).
- [48] R.J. Briggs et al., *Transport of self-focused relativistic electron beams*, in Proc of the 2nd International Topical Conf. on High Power Electron and Ion Beam (Cornell University, Ithaca NY, 3-5 oct 1977) 319.

- [49] L.I. Rudakov et al., *Behavior of large current electron beam in a dense gas*, ZhETF Pis. Red. **15** (1972) 540.
- [50] B.S. Newberger and L.E. Thode, Electrostatic two-stream instability for a scattered relativistic electron beam and collisional plasma, Phys. Fluids 25 (1982) 193.
 B.S. Newberger and L.E. Thode, A nonlinear two-stream interaction between a cold, relativistic electron beam and collisional plasma-ASTRON experiment, report LA-7814-MS (Los Alamos National laboratory, May
- [51] V.K. Grishin and V.G. Sukharevskii, *Stability of relativistic beam in dense medium*, Zh. Tekh. Fiz. **43** (1973) 887.

1979).

- [52] R. Lee and M. Lampe, *Electromagnetic Instabilities, filamentations, and focusing of relativistic electron beams*, Phys. Rev. Lett. **31** (1973) 1390.
- [53] K. Molving and G. Benford, *Filamentation instabilities of rotating electron beams*, Phys. Fluids **20** (1977) 1125.
- [54] R.C. Davidson et al., *Influence of self-fields on the filamentation instability in relativistic beam-plasma systems*, Phys. Fluids **18** (1975) 1040.
- [55] R.J. Briggs, A simple model of beam transport in low-pressure ion-focused regimes, report UCID-19187, Lawrence Livermore National Laboratory, Sept 1981.
- [56] J.R Cary et al., Simple criteria for the absence of the beam-Weibel instability, Phys. Fluids **24** (1981) 1818.
- [57] D. Finkelstein and P.A. Sturrock, *Stability of relativistic self-focusing streams*, in Plasma Physics, page 221, J.E. Drummond ed, McGraw-Hill, 1961.
- [58] H.S. Hum and M. Lampe, *Stability properties of azimuthally symmetric perturbations in an intense electron beam*, Phys. Fluids **4** (1981) 1553.
- [59] S. Weinberg, General Theory of resistive beam instabilities, J. Math. Phys. 8 (1967) 614–640. See also, J. Math. Phys. 5 (1964) 1371, and Phys. Fluids 5 (1962) 196.
- [60] E.J. Lauer et al., *Measurements of hose instability of a relativistic electron beam*, Phys. Fluids **21** (1978) 1344.

- [61] S. Jorna, and W.B. Thompson, *On the propagation of energetic ion beams through a fusion target chamber*, J. Plasma Phys. **19** (1978) 97–119.
- [62] G.J. Budker, *Relativistic Stabilized electron beam*, in CERN Symposium on High Energy Accelerators and Pion Physics, 11-23 June 1956, vol 1 page 68.
 J.G. Linhart and A. Schoch, *Relativistic electron beam devices for fusion*, Nucl. Inst. and Meth. 5 (1959) 332–345.
- [63] G.S. Kino and R. Gerchberg, *Transverse field interactions of a beam and plasma*, Phys. Rev. Lett. **11** (1963) 185.
- [64] E.P. Lee, *Hose theory*, report UCID-16268 (Lawrence Livermore National Laboratory, May 1973) 137 pp.
- [65] E.P. Lee, *Resistive hose instability of a beam with the Bennett profile*, Phys. Fluids **21** (1978) 1327.
- [66] H.S. Uhm and M. Lampe, *Theory of the resistive hose instability in relativistic electron beams*, Phys. Fluids **23** (1980) 1574.
- [67] M.N. Rosenbluth, *Long-wavelength beam instability*, Phys. Fluids **3** (1960) 932.
- [68] A.A. Ivanov and L.I. Rudakov, *Intense relativistic electron beam in plasma*, Sov. Phys. JETP **31** (1970) 715.
- [69] M. Lampe et al., *Analytic and numerical Studies of resistive Beam Instabilities*, in High-Power beams 81, Proc of the 4th International Topical Conf. on High Power Electron and Ion Beam, juin-juillet 1981, H.J. Doucet and J.M. Buzzi eds., p.145.
- [70] E.P. Lee, *Hose instability at arbitrary conductivity*, report UCID-16734, Lawrence Livermore Laboratory, March 1975.
- [71] E.P. Lee, *Sausage mode of a pinched charged particle beam*, report UCID-18940, Lawrence Livermore Laboratory, Feb 1981.
- [72] E.P. Lee et al., *Filamentation of a heavy-ion beam in a reactor vessel*, Phys. Fluids **23** (1980) 2095.
- [73] A.I. Pavlovskii et al., *The LIU-10 high-power electron accelerator*, Sov. Phys. Dokl. **25** (1980) 120.

- [74] H.L. Buchanan, *Electron beam propagation in the ion-focuses regime*, Phys. Fluids **30** 221–231.
- [75] D.P. Murphy ey al., *Interaction of an intense electron beam with preformed channels*, Phys. Fluids **30** 232–238.
- [76] K.Y. Nguyen et al., *Transverse instability of an electron beam in beam-induced ion channel*, Phys. Fluids **30** 239–241.
- [77] H.S. Uhm and R.C. Davidson, *Effects of electron collisions on the resistive hose instability in intense charged particle beams propagating through background plasma*, Phys. Rev. Spec. Topics Accel. and Beams **6** (2003) 03204-1–10.
- [78] A. Gsponer, U.S. National Missile Defense: Looking at the whole package Science **289** (8 September 2000) 1688.
- [79] J. Grinevald, A. Gsponer, L. Hanouz, and P. Lehmann, La Quadrature du CERN (Editions d'En bas, Lausanne, 1984) 186 pp.
- [80] A. Gsponer and J.-P. Hurni, *Antimatter underestimated*, Nature **325** (1987) 754.
- [81] U. Amaldi, *Spin-offs of high energy physics to society*, Int. Europhys. Conf.: High-energy physics '99 (Tampere, Finland, July 1999) 21 pp.
- [82] J. Detwiler et al., Nuclear propelled vessels and neutrino oscillation experiments, Phys. Rev. Lett. **89** (2002) 191802-1–4.
- [83] U.S. Department of Defense, *Fact sheet: Particle beam (PB) technology Program*, (U.S. Department of Defense, September 1980) 11 pp.
- [84] A. Gsponer and J.-P. Hurni, *Antimatter induced fusion and thermonuclear explosions*, Atomkernenergie–Kerntechnik **49** (1987) 198–203.
- [85] E. Hartouni, *Protons reveal the inside story*, Science and Technology Review (Lawrence Livermore National Laboratory, November 2000) 12–18.
- [86] G.S. Cunningham and C. Morris, *The development of flash radiography*, Los Alamos Science, **28** (2003) 76–91.
- [87] Subpanel recommends a collision course, CERN Courier (January/February 2002) 5.
- [88] V.G. Dudnikov, *Surface-plasma source of Penning geometry*, IVth USSR National Conf. on Particle Accelerators (1974)

- [89] G.I. Dimov and V.G. Dudnikov, A 100 mA negative hydrogen-ion source for accelerators, IEEE Trans. Nucl. Sci. 24 (1977) 1545.
- [90] E.A. Knapp and R.A. Jameson, *Accelerator technology program: July–December 1980*, Progress report LA-9131-PR (Los Alamos Scientific Laboratory, January 1982) 133 pp.
- [91] H⁻ beam emittance measurements for the Penning and the asymmetric, grooved magnetron surface-plasma sources, Proc. of the 1981 LINAC Conf., (Santa-Fe, October 19–23, 1981) 174–176.
- [92] N. Wells, *Radio frequency quadrupole and alternating phase focusing methods used in proton linear accelerator technology in the USSR*, Report R-3141-ARPA, prepared for DARPA (Rand Corporation, Santa Monica, January 1985) 70 pp.
- [93] R.A. Jameson, *Accelerator technology programme*, Status report LA-10118-SR (Los Alamos Scientific Laboratory, May 1984) 88 pp.
- [94] R.A. Jameson and R.S. Mills, *On emittance growth in linear accelerators*, Proc. of 1979 LINAC Conf., Report BNL-51134 (1979) 231–237.
- [95] J.W. Staples and R.A. Jameson, *Possible lower limit to linac emittance*, IEEE Trans. on Nucl. Sci. **NS-26** (1979) 3698–3700.
- [96] E.A. Knapp and R.A. Jameson, *Accelerator technology program: April–December 1978*, Progress report LA-8350-PR (Los Alamos Scientific Laboratory, May 1980) 198 pp.
- [97] A. Stintz et. al., Resonant Two-Photon Detachment through the Lowest Singlet D State in H⁻, Phys. Rev. Lett. **75** (1995) 2924-2927.
- [98] X.M. Zhao et al., Nonresonant Excess Photon Detachment of Negative Hydrogen Ions, Phys. Rev. Lett. **78** (1997) 1656-1659.
- [99] W. H. Kuan et al., *Photodetachment of H* $^-$, Phys. Rev. **A60** (1999) 364-369.
- [100] A. Gsponer and J.-P. Hurni, *Antimatter weapons*, Bull. of Peace Proposals **19** (1988) 444–450.
- [101] M. Thee, Antimatter technology for military purposes: excerpts from a dossier and assessments of physicists, Bull. of Peace Proposals 19 (1988) 443–470.

- [102] R.J. Burick, *Neutral particle beam research and development*, Brochure DEW-86:86 (Los Alamos Scientific Laboratory, September 1986) 14 pp.
- [103] GTA (Ground Test Accelerator) Phase 1: Baseline Design Report, LA-UR-86-2775, (Los Alamos National Laboratory, August 1986) 436 pp.
- [104] *BEAR: First neutral particle beam in space*, Research Highlights 1989 (Los Alamos National Laboratory, 1990) 24–27.
- [105] G.J. Nunz, *Beam Experiments Aboard a Rocket (BEAR) Project*. Final report. Volume 1, Project summary. Progress report LA-11737-MS-Vol-1. (Los Alamos National Laboratory, January 1990) 103 pp.
- [106] O.R. Sander et al., *Commissioning the GTA Accelerator.*, Proc. of the 16th Int. LINAC Conf., Ottawa, 23-28 August 1992. Report LA-UR-92-2716 (Los Alamos National Laboratory, NM. 1992) 6 p.
- [107] Advances in the Ground test Accelerator program, Research Highlights 1990 (Los Alamos National Laboratory, 1991) 18–19.
- [108] E. Marshall, Researcher sift the ashes of SDI, Science 263 (1994) 620–623.
- [109] J. D. Schneider, *APT Accelerator Technology*, Proc. of the LINAC 1996 Conf. (CERN, Geneva, 1996) 5 pp.
- [110] T. Rinckel, *LENS Scavengers*, Indiana University Cyclotron Facility News (March 10, 2004) 2 pp.
- [111] H.M. Harris, *Science opportunities through nuclear power in space*, CONF-950110 (American Institute of Physics, 1995) 161-167.
- [112] G.H. Canavan, *Comparison of Laser and Neutral Particle Beam Discrimination*, Report LA-11572-MS (Los Alamos National Laboratory, September 1989) 16 pp.
- [113] G. A. Mourou, C. P. J. Barty and M. D. Perry, Physics Today, 22 (January 1999).
- [114] G.H. Canavan and J.C. Browne, *Directed Energy Concepts for Theater Defense*, Report LA-12094-MS (Los Alamos National Laboratory, October 1991) 11 p.
- [115] ATA Advanced Test Accelerator (Lawrence Livermore National Laboratory, Visitor's information brochure, 1978) 16 pp.

- [116] W.A. Barletta, Generating intense electron beams for military applications, Energy and Technology Review (Lawrence Livermore National Laboratory, December 1981) 1–12.
- [117] ATA: 10-kA pulses of 50-MeV electrons, Physics Today (February 1982) 20–22.
- [118] E.G. Cook et al., *The advanced test accelerator*—A high-current induction linac, IEEE Trans. Nucl. Sci. **NS-30** (1983) 1381–1386.
- [119] C.H. Jackson et al., *The Advanced Test Accelerator (ATA) injector*, IEEE Trans. Nucl. Sci. **NS-30** (1983) 2725–2727.
- [120] L. Reginator et al., *The Advanced Test Accelerator (ATA), a 50-Mev, 10-kA induction linac*, IEEE Trans. Nucl. Sci. **NS-30** (1983) 2970–2974.
- [121] J.M. Peterson, *Betatron with kiloamper beams*, IEEE Trans. Nucl. Sci. NS-30 (1983) 1396–1398.
- [122] N.C. Christofilos, et al., *High current linear induction accelerators for electrons*, Rev. Sci. Inst. **35** (1964) 886–890.
- [123] W.E. Martin et al., *Electron-beam guiding and phase-mix damping by a laser-ionized channel*, Phys. Rev. Lett. **54** (18 February 1985) 685–687.
- [124] Particle-beam research, New Scientists (21 March 1985) 18.
- [125] D.S. Prono and G.J. Caporaso, *Electrostatic channel guiding: A technological breakthrough*, Energy and Technology Review (Lawrence Livermore National Laboratory, March 1985) 1–11.
- [126] D.S. Prono et al., *Recent progress of the Advanced Test Accelerator*, IEEE Trans. Nucl. Sci. **NS-32** (October 1985) 3144–3148.
- [127] G.J. Caporaso et al., *Laser guiding of electron beams in the Advanced Test Accelerator*, Phys. Rev. Lett. **57** (29 September 1986) 1591–1594.
- [128] R.B. Miller, *Stabilizing electron beams*, Nature **325** (8 January 1987) 105–106.
- [129] R. Batzel, *The State of the Laboratory*, Energy and Technology Review (Lawrence Livermore National Laboratory, July 1987) 1-3.
- [130] *Beam Research*, Energy and Technology Review (Lawrence Livermore National Laboratory, July 1987) 54–55.

- [131] B. Hui and Y.Y. Lau, *Injection and extraction of a relativistic electron beam in a modified betatron*, Phys. Rev. Lett. **53** (19 November 1984) 2024–2027.
- [132] J.J. Petillo and R.C. Davidson, *Kinetic equilibrium and stability properties of high-current betatrons*, Phys. Fluids. **30** (1987) 2477–2495.
- [133] W.A. Barletta, *Electron accelerators with pulsed power drives*, Proc. Eur. Accel. Conf. (Nice, France, 1990) 186–190.
- [134] A. Heller, *Breakthrough design for accelerators*, Science and Technology Review (Lawrence Livermore National Laboratory, October 1999) 10-11.
- [135] A.I. Pavlovskii and V.S. Bossamykin, *Linear inductive accelerator without iron*, Atomnaya Energia **37** (1974) 228–233.
- [136] A.I. Pavlovskii et al., *Pulsed air-cored betatrons powered from magnetocumulative generators*, Atomnaya Energia **41** (1976) 142–144.
- [137] R.B. Miller et al., *Multistage linear acceleration using pulsed transmission lines*, J. Appl. Phys. **52** (1981) 1184–1186.
- [138] C.A. Kapetanakos and P. Sprangle, *Ultra-high-current electron induction accelerators*, Physics Today (February 1985) 58–69.
- [139] R.B. Miller, *RADLAC technology review*, IEEE Trans. Nucl. Sci. **NS-32** (1985) 3149–3153.
- [140] M.G. Mazarakis et al. *Experimental investigation of beam generation, acceleration, transport, and extraction in the RADLAC-II pulsed transmission line linear accelerator*, Report SAND-86-1240C (Sandia National Laboratory, 1986) 13 pp.
- [141] D.E. Hasti, *RADLAC summary*, DARPA Conference, Albuquerque, NM. 23 June 1986, Report SAND-86-1593C (Sandia National Laboratory, 1986) 6 pp.
- [142] D.E. Hasti, Endoatmospheric Propagation Experiments and Accelerator Development., SDIO/DARPA Services Annual Propagation Review, Monterey, CA. 29 September 1987, Report SAND-87-2341C (Sandia National Laboratory, 1987) 4 pp.
- [143] V.S. Bossamykin et al., *Linear induction accelerator LIA-10M*, Proc. of the 9th IEEE Int. Pulsed Power Conf. (Albuquerque, NM, June 21–23, 1993) 905–907.

- [144] S. Kassel and C.D. Hendricks, *High-current particle beams: I. The western USSR research groups*, Report R-1552-ARPA, prepared for DARPA (Rand Corporation, Santa Monica, April 1975) 110 pp.
- [145] N. Wells, Soviet research on the transport of intense relativistic electron beams through low-pressure air, Report R-3309-ARPA, prepared for DARPA (Rand Corporation, Santa Monica, August 1986) 51 pp.
- [146] R.J. Fahel et al., *Sparking limits, cavity loading, and beam breakup instability with high-current RF linacs*, Report LA-9126-MS (Los Alamos National Laboratory, January 1982) 21 pp.
- [147] T.J. Boyd et al., *PHERMEX* A high-current accelerator for use in dynamics radiography, Rev. Sci. Inst. **36** (1965) 1401–1408.
- [148] D.C. Moir et al., *Intense electron-beam propagation in low-density gases using PHERMEX*, Report LA-UR-80-3260 (Los Alamos National Laboratory, 1980) 33 pp.
- [149] T.P. Starke, *PHERMEX standing-wave linear accelerator*, IEEE Trans. Nucl. Sci. **NS-30** (1983) 1402–1404.
- [150] D.C. Moir et al., *Time-resolved, current-density, and emittance measure-ments of the PHERMEX electron beam*, IEEE Trans. Nucl. Sci. **NS-32** (1985) 3018–3020.
- [151] D.C. Moir and G.R. Gisler, *PHERMEX as an injector to a modified betatron*, Report LA-UR-85-3739 (Los Alamos National Laboratory, 1985) 4 pp.
- [152] G.R. Gisler, *Particle-in-cell simulations of azimuthal instabilities in relativistic electron layers*, Phys. Fluids **30** (1987) 2199–2208.
- [153] I.S. Roth et al., *High current ion beam generation and transport system*, Appl. Phys. Lett. **46** (1985) 251–253.
- [154] D. Neuffer, $\mu^+ \mu^-$ colliders, Report CERN-99-12 (CERN, Geneva, 1999) 76 pp.
- [155] W.A. Barletta and A.M. Sessler, Stochastic cooling in muon colliders, in J. Bosser, Ed., Workshop on beam cooling and related topics, Montreux, 4—8 October 1993, Report CERN-94-03 (CERN, Geneva, 1994) 145–151.
- [156] W.A. Barletta, Free-electron laser for strategic defense: The benefits of open scientific exchange, Report UCRL-94166 (Lawrence Livermore National Laboratory, 1986) 5 pp.

- [157] S. Geer, Muon cooling R&D, Nucl. Inst. Meth. **A503** (2001) 64–69.
- [158] S. Geer and A. Gsponer, *Radiation dose distributions close to the shower axis calculated for high energy electron initiated electromagnetic showers in air*, Atomkernenergie–Kerntechnik **4** (1983) 42–46.